lysates were transferred to 96-well plates, and Luc$^+$ and *R*luc luminescence was measured using the Dual-Luciferase Reporter Assay System (Promega) in the Wallac Arvo SX Multi-Label counter. Transfection and translation efficiencies varied between independent experiments, and the results were normalized by calculating Luc$^+$/*R*luc ratios. All assays were performed in triplicate.

Immunoblotting. Immunoblotting was performed to evaluate expressed AhR protein levels after transient transfection experiments. Cells plated in six-well plates were washed with phosphate-buffered saline, lysed in 0.5 ml of SDS lysis buffer (1% SDS, 10 mM EDTA, and 50 mM Tris-HCl, pH 8) containing Complete Protease Inhibitor Cocktail (Roche, Basel, Switzerland) and sonicated to shear DNA. Protein concentration in the cell lysates was measured by the Bradford method using a Bio-Rad Protein Assay (Bio-Rad Laboratories, Munich, Germany), and 20-μg aliquot of each sample was separated on an SDS-polyacrylamide gel. Immunoblotting for AhR was performed as described previously (Pollenz et al., 1994) with anti-human AhR antibody (SA-210; Biomol GmbH, Hamburg, Germany). Detection was performed with peroxidase-labeled anti-rabbit antibody using the ECL Plus detection system (GE Healthcare Bio-Sciences, Uppsala, Sweden). The bands were visualized and imaged using ChemiDoc XRS Plus (Bio-Rad Laboratories).

Generation of Stable Cell Lines Expressing Mutant AhRs. The pCI-neo plasmids containing mouse and rabbit AhR cDNAs with point mutations were transfected into c12 cells. Stable transformants expressing AhRs were selected by using G418 and screened for ethoxyresorufin-*O*-deethylase activity as described previously (Kennedy and Jones, 1994) after treatment with 10 nM TCDD. We chose and mixed more than six representative clones from transformants obtained with each plasmid and investigated CYP1A1 inducibility by TCDD and OME using real-time reverse-transcription polymerase chain reaction methods. In brief, the cells plated in six-well plates at 80% confluence were exposed to 50 μM OME or 10 nM TCDD. After 12 hours of exposure, total RNA was isolated using Isogen (Nippon Gene, Tokyo, Japan) according to the manufacturer's instructions. An aliquot (2 μg) of total RNA was subjected to RT using MultiScribe RT (Applied Biosystems, Foster City, CA) and oligo-dT primers. An aliquot of cDNA (2 μl) or calibrator plasmid DNA (pCI-neo-mAhR) was amplified with master mixture (SYBR Premix Ex Taq; Takara Bio, Kyoto, Japan) containing gene-specific primers. The primer pair for mouse CYP1A1 cDNA amplification is shown in Supplemental Table 1. The reaction mixture was amplified using the Smart Cycler System (Cepheid; Takara Bio) under the following conditions: an initial incubation at 95°C for 15 minutes, followed by 40 cycles of 95°C for 15 seconds, 60°C for 20 seconds, and 72°C for 10 seconds. To confirm amplification specificity, the PCR products were subjected to melting curve analyses. A calibration curve was generated by threshold

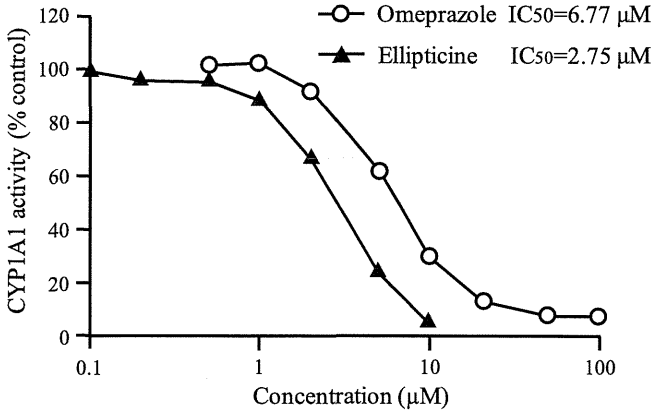

Fig. 1. Inhibition of human CYP1A1 activity by omeprazole. CYP1A1 activity was determined using P450-Glo Assays and Sf9 cell microsomes containing recombinant human CYP1A1. Luciferin-CEE (a specific substrate for CYP1A1) and microsomes were incubated at 37°C for 30 minutes with various concentrations of omeprazole or ellipticine. Each data point represents the mean of duplicate determinations.

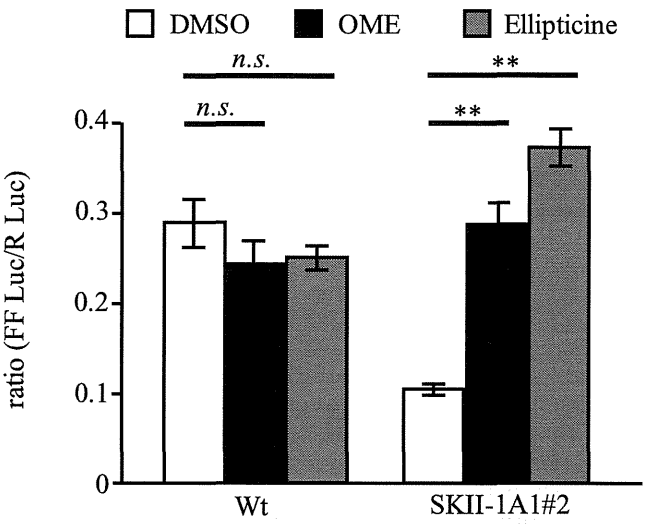

Fig. 2. OME restores XRE-dependent transcription in CYP1A1-overexpressing SKII-1A1 cells and CYP1A1-deficient SK-Hep-1 cells. CYP1A1-deficient SK-Hep-1 (Wt) and its derivative cell lines overexpressing CYP1A1 (SKII-1A1#2) cultured in medium containing 10% FBS were transfected with the 4xXRE-Luc reporter gene and pCMV-Rluc. After transfection, fresh medium containing 100 μM omeprazole (closed column), 5 μM ellipticine (gray column) or dimethylsulfoxide (DMSO) (solvent control, open column) was added. Data are represented as the ratio of firefly luciferase activity to *Renilla* luciferase activity observed 16 hours after OME was added. (FFluc/*R*luc, mean ± S.D., n = 3) (**P < 0.01, n.s., no significant difference to control). FFluc, firefly luciferase.

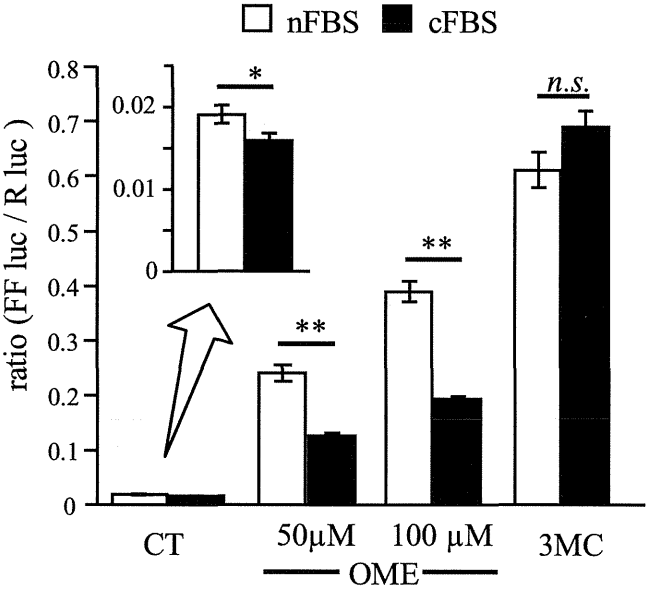

Fig. 3. Effects of FBS on XRE-dependent transcriptional activation. HepG2 cells were transfected with the 4xXRE-Luc reporter gene and pCMV-Rluc. After transfection, the culture medium was changed to fresh DMEM containing normal FBS (nFBS, open column) or charcoal-stripped FBS (cFBS, closed column). Twenty-four hours after medium exchange, dimethylsulfoxide (solvent control; CT), 50 or 100 μM OME was added. Significant reductions in OME-induced transcription was noted with charcoal stripping; however, 3MC (1 μM)-induced transcription was not affected. Data are represented as mean ± S.D. (n = 3) 16 hours after OME addition. (*P < 0.05; **P < 0.01; n.s., no significant difference). FFluc, firefly luciferase.

cycles of calibrators of a known plasmid copy number. The initial quantity of target mRNA in the samples was determined by correlating their threshold cycles to the calibration curve.

Results

OME Inhibits CYP1A1 Activity. To examine whether OME directly inhibits CYP1A1 activity, recombinant human CYP1A1 proteins expressed by Sf9 cells were used in the inhibition study. In addition to ellipticine, a typical CYP1A1 inhibitor, OME also inhibited CYP1A1 activity. The mean inhibitory concentration value was 6.77 μM in case of OME and 2.75 μM in ellipticine (Fig. 1, data re-examined as reported in our previous study, Shiizaki et al., 2008). CYP1A1 activity was inhibited nearly 90% by more than 20 μM of OME, and this concentration correlated to the concentration of OME required for AhR activation (Diaz et al., 1990; Dzeletovic et al., 1997).

We confirmed species-specific induction of CYP1A1 by OME (Supplemental Fig. 1A). Induction of CYP1A1 mRNA by OME occurred not only in human hepatoma HepG2 cells but also in mouse Hepa1c1c cells (Kikuchi et al., 1995). This induction was well correlated with XRE-driven reporter gene induction (Supplemental Fig. 1B). We used this reporter assay system to evaluate OME-mediated AhR activation, which, consequently, led to CYP1A1 induction.

OME Restores XRE-Dependent Transcription in CYP1A1-Overexpressing SKII-1A1 Cells and CYP1A1-Deficient SK-Hep-1 Cells. As reported in our previous study, in the presence of 10% FBS, the human hepatoma cell line SK-Hep-1, which is deficient in *CYP1A1* expression, showed higher basal transcription from the XRE-driven reporter gene without additional exogenous ligands than other human hepatoma cells (Shiizaki et al., 2005). We compared basal transcription levels of CYP1A1-overexpressing cell lines (SKII-1A1 cells) and found that basal transcription levels in these cells were significantly lower than those in wild-type SK-Hep-1 cells. Using this reporter system, OME or ellipticine was added to culture media of the wild-type SK-Hep-1 and SKII-1A1#2 cells (one of the CYP1A1-overexpressing clones). OME restored the transcription in the SKII-1A1#2 cells to a level similar to that in the wild-type cells (Fig. 2). Treatment of CYP1A1 inhibitor ellipticine indicated similar results. These observations suggest that OME does not transactivate XRE-driven reporter genes directly via AhR activation but instead inhibits transcription repression by CYP1A1 activity.

Charcoal-Stripping of Serum Diminished the Basal Transcription Level and OME-Induced Transcription of the XRE-Driven Reporter Gene in HepG2 Cells. Next, we tested the effect of FBS on the transcription induction of XRE-driven reporter genes by OME to provide indirect evidence of the presence of substances in FBS that might transactivate AhR. The human hepatoma cell line HepG2 and SK-Hep-1 cells are similar in terms of the expression levels of AhR and Arnt molecules (Shiizaki et al., 2005). The 4xXRE-Luc reporter gene and pCMV-Rluc were cotransfected into HepG2 cells. After transfection, the culture medium was changed to fresh DMEM containing normal FBS or charcoal-stripped FBS. Although OME-induced transcription was clearly observed in DMEM containing normal FBS, significantly less OME-induced transcription was observed in DMEM containing charcoal-stripped FBS (Fig. 3). Charcoal-stripping of FBS did not reduce 3MC (1 μM)-induced transcription. Together with this and the previously mentioned results (Figs. 1 and 2), it is highly suspected that OME-mediated AhR activation of the XRE-dependent gene is due to the inhibition of the activity of CYP1A1 enzymes, which may metabolize putative AhR ligands contained in FBS.

Comparison of the Responses of AhRs Derived from Various Mammals to OME. While exploring the genes that cause species-specific susceptibility against dioxin, we prepared six AhR expression plasmids from six mammalian species using pCI-neo vectors. In these experiments, we used HeLa cells, which possess *CYP1A1* and express a similar level of ARNT molecules and a lower level of AhR molecules compared with HepG2 or SK-Hep-1 cells. We also used mouse

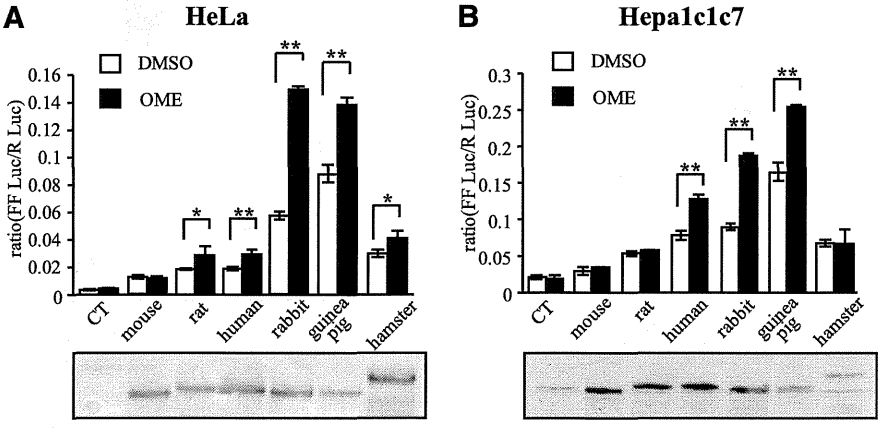

Fig. 4. Comparison of the induction of XRE-dependent transcription by OME through six mammalian AhR species. HeLa (A) and Hepa1c1c (B) cells were transfected with an empty vector (pCI-neo, CT, negative control) or six mammalian AhR expression plasmids (generated from the mouse, rat, human, rabbit, guinea pig, and hamster) together with the XRE-driven pX4TK-Luc reporter gene and pCMV-Rluc. After 24 hours, the cells were exposed to 100 μM OME or 0.1% dimethylsulfoxide (DMSO). After 16 hours of incubation, the cells were lysed, and firefly luciferase and *Renilla* luciferase activities were measured. Data represent the mean ± S.D. of normalized firefly luciferase (FFluc)/*Renilla* luciferase activities of three independent experiments. OME-treated groups (closed columns) were compared with DMSO controls (open columns) using one- or two-way analysis of variance, and statistically significant differences are denoted by asterisks ($^*P < 0.05$; $^{**}P < 0.01$). Total cell lysates were subjected to immunoblotting to confirm the expression level of each AhR (lower panels).

hepatoma Hepa1c1c7 cells, which expressed a sufficient level of AhR. During this project, we used OME in addition to TCDD to examine the species-specific influence on AhR-dependent transcription. XRE-driven reporter gene assays were performed by cotransfection of the previously mentioned six AhR expression vectors and 4xXRE-Luc reporter genes.

The constitutive transcription of XRE-dependent luciferase differed among AhR species expressed in HeLa and Hepa1c1c7 cells (Fig. 4, A and B). Although overexpressed AhR protein levels were almost similar in HeLa cell experiments, the highest basal transcription level was detected in the guinea pig AhR, followed by the rabbit AhR (Fig. 4A). The pattern of basal transcription levels with each AhR in the Hepa1c1c7 cell experiments was similar to those in the HeLa cells; however, the levels did not correlate with the protein levels measured by immunoblotting (Fig. 4B). Of the six AhRs, the mouse AhR transfection caused the least increment in constitutive activity in both cells, as well as no significant induction of genes with the addition of OME (Fig. 4, A and B). Considering the effects of exogenous AhRs transfection, reporter gene induction by OME was highest when the rabbit AhR was used, followed by the guinea pig AhR (Fig. 4, A and B). However, in addition to the mouse AhR, rat and hamster AhRs were not activated by OME in mouse hepatoma cells. These results suggest that transcriptional activation by OME was dependent on the AhR species as well as the species of host cells.

Responses of Chimeric AhRs to OME. According to our already described observations, we speculated that the rabbit AhR must contain a domain responsible for OME-induced XRE-dependent transcription. Six chimeric AhRs were constructed using mouse and rabbit AhR cDNAs (Fig. 5A). Among the chimeric constructs, MR1, RM2, and MRM1, which included the rabbit LBD (amino acids 261–393), showed OME-dependent reporter gene induction. MR2, RM1, and RMR1, which included the mouse LBD (amino acids 257–389), did not respond to OME, despite the other regions of these chimeras were of the rabbit AhR (Fig. 5A). To determine the minimum requirement for the response to OME, chimeric AhRs were constructed with half LBDs; however, no constructs with partial rabbit AhR LBDs responded to OME (Fig. 5B). These data suggest that the response to OME required the complete rabbit AhR LBD and that multiple amino acid combinations specific to the rabbit AhR should be indispensable for OME-mediated AhR activation.

Determination of the Amino Acid Residues Responsible for OME-Mediated AhR Activation. Next, we conducted a study of a single amino acid substitution in the rabbit AhR that would eliminate OME-mediated AhR activation. There are 16 amino acid differences between the rabbit and mouse AhR LBDs (Fig. 6A). As shown in Fig. 6B, the basal transcriptional activity of rabbit AhR mutants was variously changed by a single amino acid substitution. Most of the mutants, except M328I, T353A, and F367L, did not much influence the OME-mediated transcriptional level. These three mutants reduced induction to less than one half of wild-type rabbit AhR, which showed an approximately 3-fold change by OME. The OME-mediated inductive ratio of M328I, T353A, and F367L was 1.7-, 1.2-, and 1.0-fold, respectively. Difference in properties between mouse AhR and rabbit AhR is the basal transcriptional activity and OME-induced transcriptional activity. By plotting these properties to emphasize differences of AhR mutants, we found the three mutant AhRs—M328I, T353A, and F367L—indicated intermediate properties of the mouse AhR and rabbit AhR (Fig. 6C).

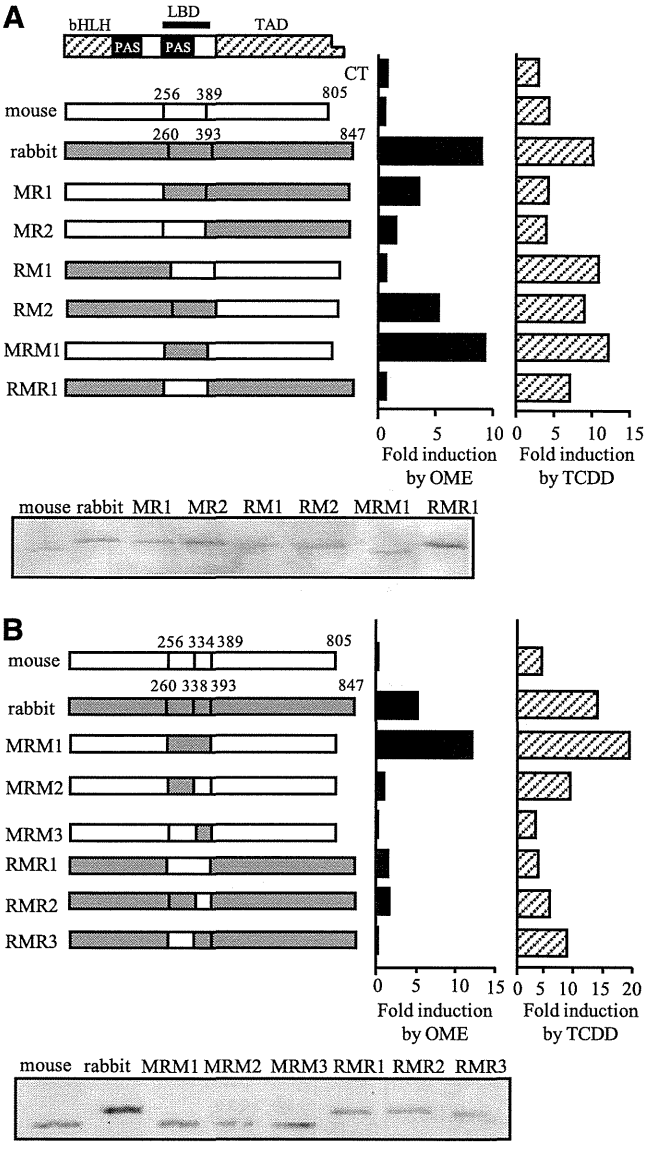

Fig. 5. Construction of chimeric AhRs and their responses to OME and TCDD. (A) Schematic diagrams of the six chimeric constructs (MR1, MR2, RM1, RM2, MRM1, and RMR1) generated from parts of cDNAs of the rabbit (white) and mouse AhRs (gray) for the first screening. HeLa cells were transfected with expression plasmids containing chimeric AhRs or the empty vector (CT, negative control) together with pX4TK-Luc and exposed to 100 μM OME, 10 nM TCDD, or 0.1% dimethylsulfoxide (DMSO). Induction of the reporter gene by these chimeric AhRs after exposure to OME (left) and TCDD (right). Data represent means of the fold induction above the control from two independent experiments. Immunoblotting was performed to confirm the expression level of each AhR (lower panel). (B) The second screening to narrow the responsible domain. Four more chimeric constructs (MRM2, MRM3, RMR2, and RMR3) were generated and subjected to the same assay. Immunoblotting was performed to confirm the expression level of each AhR (lower panel).

In addition, we constructed double and triple substitutions of these three amino acid residues in the rabbit AhR. As shown in Fig. 7A, the combinations of M328I and T353A or

A

```
Mouse  257 LALFAIATPLQPPSILEIRTKNFIFRTKHKLDFT 290
Rabbit 261 ********************************** 294

Mouse  291 PIGCDAKGQLILGYTEVELCTRGSGYQFIHAADI 324
Rabbit 295 *T*******IV******A***M***********M 328

Mouse  325 LHCAESHIRMIKTGESGMTVFRLLAKHSRWRWVQ 358
Rabbit 329 *Y***************LA*****T*DN**A*** 362

Mouse  359 SNARLIYRNGRPDYIIATQRPLTDEEGREHL    389
Rabbit 363 ****F**K*****F**************     393
```

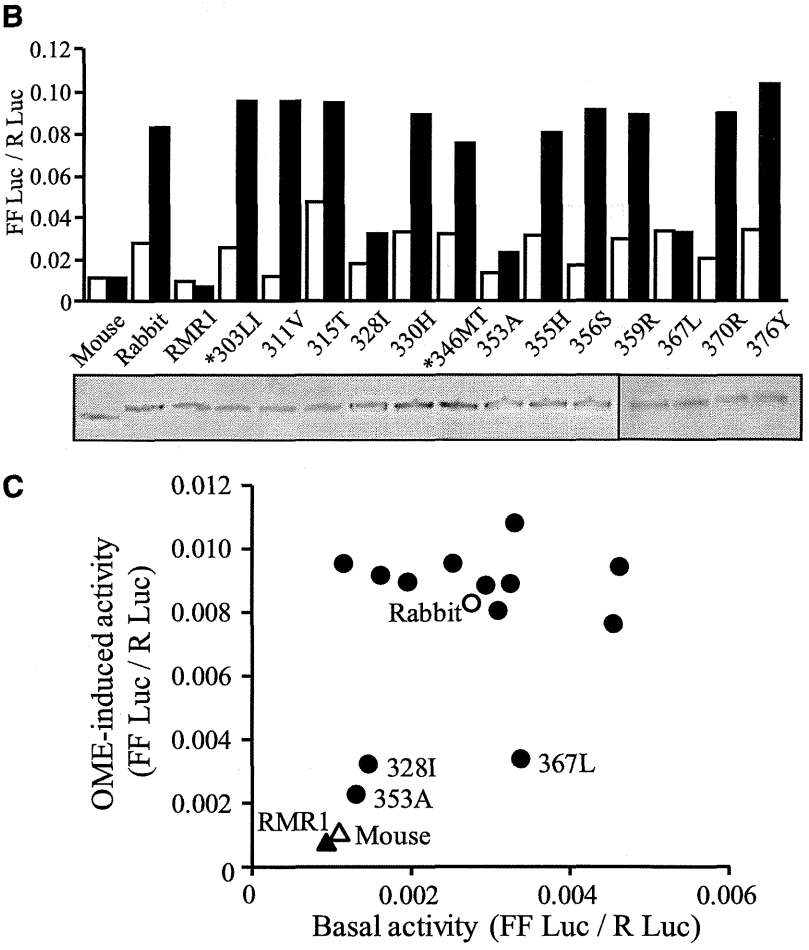

Fig. 6. Effects of point mutations on the response of the rabbit AhR to OME. (A) Amino acid alignment of mouse and rabbit AhR LBDs. Identical amino acid residues are indicated by asterisks. Differing amino acids are indicated in bold. Underlined sequences indicate the overlapping sequence for connecting with the mouse and rabbit LBDs shown in Fig. 5B. (B) Amino acids within the rabbit AhR LBD were individually replaced with the corresponding amino acids of the mouse AhR. RMR1 is the construct as shown in Fig. 5A. Asterisks indicate the mutated AhR in which two adjacent amino acids were replaced simultaneously. HeLa cells were transfected with expression plasmids containing mutated AhRs, pX4TK-Luc, and pCMV-Rluc. After 24 hours, the cells were exposed to 100 μM OME or 0.01% dimethylsulfoxide (DMSO) for 16 hours. Data represent the means of normalized firefly luciferase/*Renilla* luciferase activities of two independent experiments. Total cell lysates were prepared 24 hours after transfection and analyzed using immunoblotting to confirm the expression level of each AhR (lower panels). (C) The relationship between basal transcriptional activity and the OME-mediated transcriptional activity were plotted. ○, wild-type rabbit AhR; ●, rabbit AhR mutants; △, wild-type mouse AhR; ▲, RMR1 chimera AhR.

T353A and F367L substitutions impaired OME-mediated transcriptional induction. Moreover, the triple substitutions of M328I, T353A, and F367L exhibited properties that were remarkably similar to those of the mouse AhR (i.e., low constitutive activity and OME unresponsiveness). In contrast, mouse AhRs with single amino acid substitutions of I324M, A349T, or L363F, which are residues equivalent to M328, T353, and F367 in the rabbit AhR, slightly introduced OME responsiveness with increased levels of constitutive activities (Fig. 7B). However, triple substitutions of these three residues in the mouse AhR resulted in an approximately 5-fold induction by OME, which was not observed in wild-type mice.

Among the three amino acids, we focused on rabbit F367 because this residue is rabbit-specific (Fig. 8A). In addition, the guinea pig AhR was as responsive to OME as the rabbit AhR, and the amino acid corresponding to rabbit F367 is V368 in the guinea pig AhR, which is different in the other four species (Leu). Therefore, we constructed several mutated mouse and guinea pig AhRs to confirm that Val in this position was effective for the response to OME. As shown in Fig. 8B, the mouse AhR with triple substitutions of L363V, I324M, and A349T responded more to OME compared with double substitutions of I324M and A349T. In contrast, the response of the guinea pig AhR to OME was abolished by the V368L substitution. These results suggest that the combination of three amino acid residues of the AhR (i.e., Met, Thr, and Phe) are required for the response to OME) and also that Phe can be replaced with Val. The importance of these three amino acid residues in the OME response was confirmed by human AhR mutants as well as guinea pig AhR (Supplemental

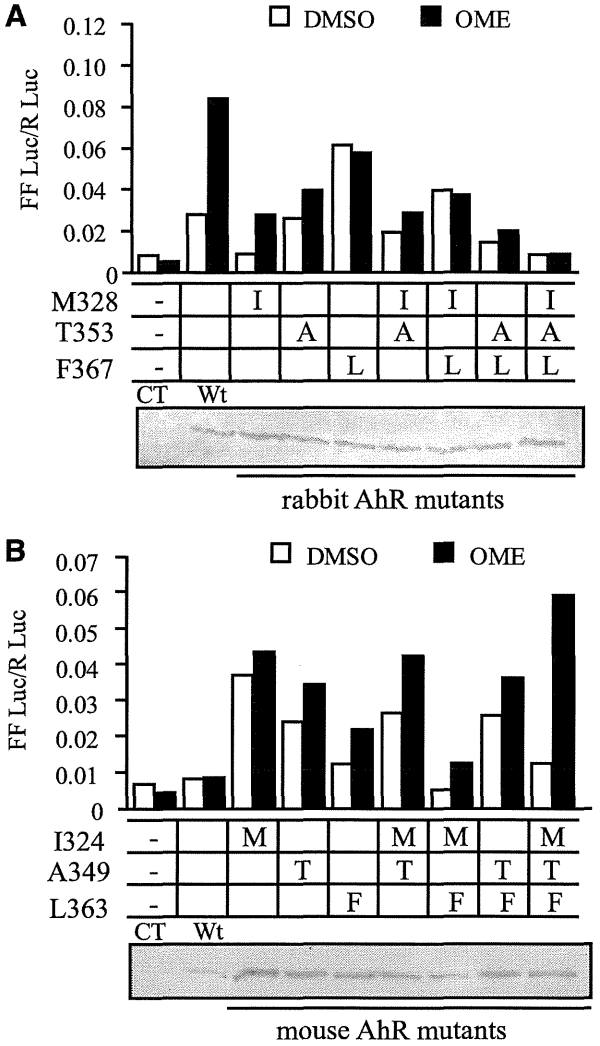

Fig. 7. Effect of single, double, and triple mutations on the response of rabbit and mouse AhRs to OME. (A) Rabbit AhRs with combinations of the three mutations of M328I, T353A, and F367L were transfected into HeLa cells along with the reporter genes. The combinations of the three mutations are indicated in the bottom table of the graph. I, 328Ile; A, 353Ala; L, 367Leu; CT, empty expression vector; Wt, wild-type rabbit AhR. The cells were exposed to 100 μM OME or 0.01% dimethylsulfoxide (DMSO) for 16 hours. Data represent the means of normalized firefly luciferase (FFluc)/*Renilla* luciferase activities of two independent experiments. (B) Mouse AhRs with combinations of the three mutations of I324M, A349T, and L363F were prepared, and luciferase assays were performed as described above. The combinations of the three mutations are indicated in the bottom table of the graph. M, 324Met; T, 349Thr; F, 363Phe; Wt, wild-type mouse AhR. Total cell lysates were prepared 24 hours after transfection and analyzed using immunoblotting to confirm the expression level of each AhR (lower panels).

Fig. 2). When two amino acid residues (330M and 355T) in human AhR were changed to mouse-type amino acid (330I and 355A), OME response was attenuated. Contrary to this, 369F, which is particularly in rabbit AhR, represent higher OME-response than wild-type human AhR.

CYP1A1 Gene Induction by OME Restored the Three Amino Acid Substitutions in the Mouse AhR and Abolished Them in the Rabbit AhR. To confirm the results that M328, T353, and F367 in the rabbit AhR are responsible for the OME-mediated AhR activation, we established cell lines that stably expressed AhRs, including the triple point mutations. The c12 cell line, which is a Hepa1c1c-derived subline lacking endogenous AhR expression, was used for this purpose and examined for CYP1A1 induction by TCDD or OME exposure. As shown in Fig. 9, CYP1A1 mRNA induction by OME was similar to that observed in the reporter assays (Fig. 7); that is, the induction was limited to the cells expressing the wild-type rabbit AhR or the mouse AhR with the three amino acid substitutions. TCDD-induced CYP1A1 mRNA induction was observed at similar levels in all cell lines expressing both wild-type and mutated AhRs, suggesting that TCDD-induced AhR activation was not influenced by these amino acid substitutions.

Responses of Mutated AhRs to Typical AhR Ligands. Next, we characterized the responses of the mutated AhRs to typical AhR ligands, including AhRs with substitutions of the three amino acids involved in the response to OME. As shown in Fig. 10 and Table 1, EC_{50} values calculated from the dose-response curves of three typical chemical ligands were slightly changed (within 2-fold) by these three amino acid substitutions that drastically reversed OME responsiveness. We also tested candidates for endogenous ligands, namely, ITE (Song et al., 2002), FICZ (Wei et al., 1998), indirubin (Adachi et al., 2001), and kynurenic acid (DiNatale et al., 2010), which have induction potencies that differ between mouse and rabbit AhRs. FICZ induced transcriptional activity at a lower concentration with the rabbit AhR than with the mouse AhR, whereas indirubin had a reverse effect. However, as with the chemical ligands, the dose-response curves and EC_{50} values for the putative endogenous ligands were not much changed by the three amino acid substitutions. (Fig. 11; Table 1). These results show that these three amino acid residues define OME sensitivity but do not influence the responsiveness of the other AhR ligands tested in this study.

Discussion

This study aimed to identify and experimentally validate the factor(s) generating species-specific responsiveness of AhR to OME. First, we speculated that OME-mediated AhR activation is due to increasing amounts of putative AhR ligands resulting from the inhibition of CYP1A1 activity by OME. This hypothesis is based on the following observations: 1) OME-mediated AhR activation required CYP1A1 activity and was influenced by endogenous ligands included in serum. 2) The concentration of OME activating AhR was higher than with that of the typical AhR ligand and was similar to the concentration of OME required for CYP1A1 inhibition. 3) The comparison of AhRs from six mammalian species revealed that transcriptional activation of the reporter gene by OME seemed to correlate with the basal transcription level, reflecting the response of the putative endogenous ligand. If a type of ligand mediates OME-dependent AhR activation, OME responsiveness would be attributable to the AhR itself, independent of host cells. In the present study, we constructed chimeric AhRs from mouse and rabbit AhRs, which indicated that OME responsiveness required multiple amino acid residues present in the LBD of the rabbit AhR. These amino acid residues were not present in the mouse AhR. In conclusion, we demonstrated that M328, T353, and F367 of the rabbit AhR were required for OME responsiveness.

These results are fundamentally different from those of previous reports on cell-specific factors that define OME

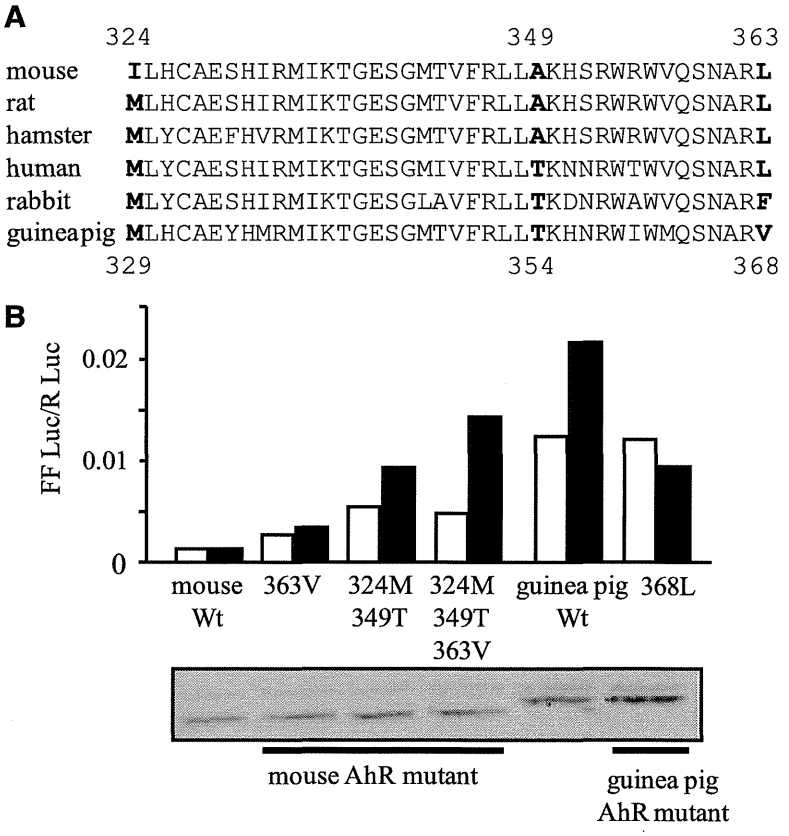

Fig. 8. Effect of single, double, and triple mutations on the response of mouse and guinea pig AhRs to OME. (A) Alignment of the LBD amino acid sequences for six mammalian AhRs. The numbers indicate the amino acid positions in the mouse AhR (top line) and guinea pig AhR (bottom line). The three candidate amino acids that are crucial for the response to OME are in bold font. (B) Mouse AhRs with combinations of the three mutations and the guinea pig AhR with the V368L substitution were transfected into HeLa cells along with the reporter genes. Wt, wild-type mouse AhR or wild-type guinea pig AhR. The cells were exposed to 0.01% dimethylsulfoxide (DMSO) or 100 μM OME for 16 hours. Data represent the means of normalized firefly luciferase (FFluc)/*Renilla* luciferase activities of two independent experiments. Total cell lysates were prepared 24 hours after transfection and analyzed using immunoblotting to confirm the expression level of each AhR (lower panel).

responsiveness (Kikuchi et al., 1995, 2002; Dzeletovic et al., 1997). Some of the differences may be due to the species used because most of the mentioned studies used the human AhR, whereas we primarily used the rabbit AhR, which is highly sensitive to OME. In a previous report (Dzeletovic et al., 1997), the human AhR transiently expressed in mouse hepatoma c12 cells was not activated by OME. We performed a similar experiment with c12 cells stably expressing the rabbit AhR, and these cells exhibited inducible expression of CYP1A1 by OME (Fig. 9). We thought the stably expressed rabbit AhR altered intracellular conditions (e.g., the basal level of CYP1A1 expression) to respond to the AhR activator. In fact, the c12-derived cells expressing the rabbit AhR exhibited a raised level of constitutive CYP1A1 expression and remarkable CYP1A1 induction (>15-fold) on TCDD exposure.

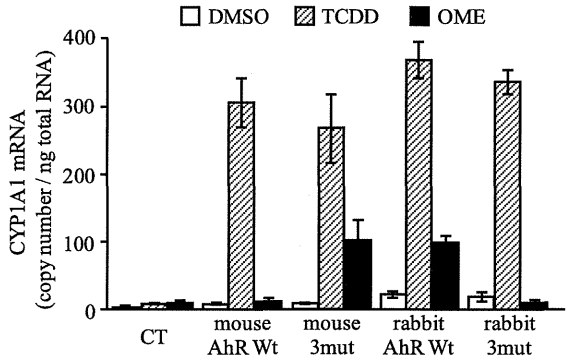

Fig. 9. CYP1A1 mRNA induction by OME in stable transformants of mutant AhRs. AhR-deficient mouse hepatoma c12 cells were transfected with the expression vector of the mouse AhR, rabbit AhR, their derivative mutated AhRs. Mouse 3mut, mouse AhR with I324M, A349T, and L363F substitutions or pCI-neo empty vector (CT, negative control). Rabbit 3mut, rabbit AhR with M328I, T353A, and F367L substitutions. After transfection, a heterogeneous population of G418-resistant cells was maintained and exposed to 0.1% dimethylsulfoxide (DMSO) (solvent control), 10 nM TCDD, or 100 μM OME. After 16 hours of incubation, total RNA was isolated, and mouse CYP1A1 mRNA was measured using real-time reverse-transcription polymerase chain reaction as described in *Materials and Methods*. Data represent mean ± S.D. (n = 3).

Several investigations have identified specific amino acid residues that are important for AhR activation. We previously reported that L318 in the mouse AhR is required for the response to β-naphthoflavone (Goryo et al., 2007). An AhR polymorphism (A375V) in C57BL/6 and DBA/2 mice results in a difference in TCDD binding affinity and consequent toxicity (Ema et al., 1994). Two polymorphisms, V325I and A381S, in the common tern and chicken AhRs are responsible for sensitivity to TCDD (Karchner et al., 2006). Interestingly, the V325I polymorphism in the bird species corresponds to the mouse AhR I324, one of the critical amino acids for OME responsiveness. In the tern AhR, Ile is required in this position for high sensitivity to TCDD. The single mutation I324M in the mouse AhR was insufficient for producing a response to OME but instead increased basal transcriptional activity. The amino acid residue at this position could be close to TCDD and may be one of the key amino acids for ligand binding and constitutive activity. As mentioned in *Results*, F367 is specific to the rabbit AhR. In the guinea pig AhR, the corresponding amino acid is V363, and the L363V substitution was an

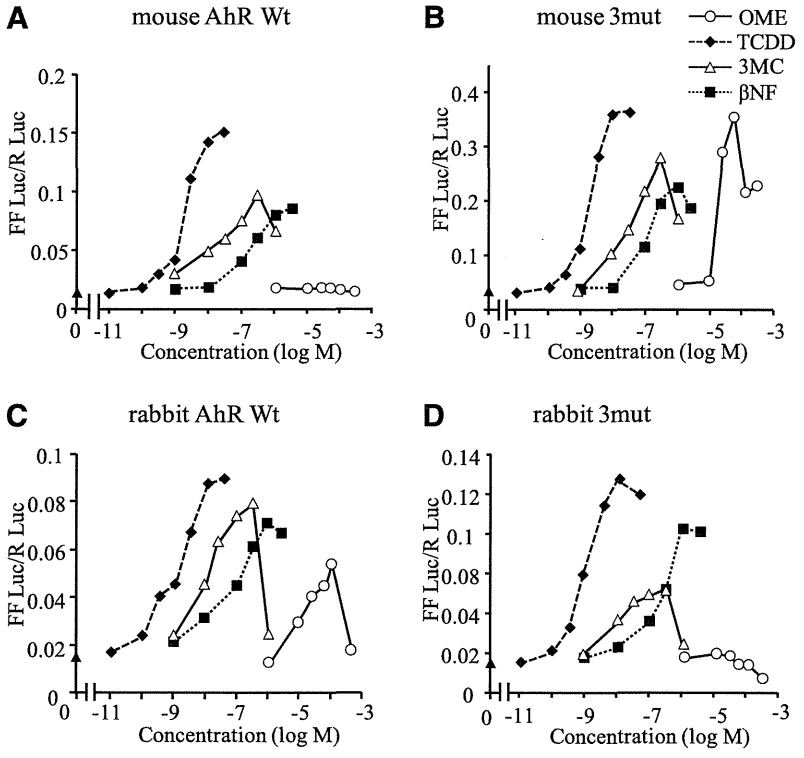

Fig. 10. Response of mouse and rabbit AhR mutants to OME, TCDD, 3MC, and β-naphthoflavone (β-NF). HeLa cells were transfected with reporter genes and (A) the mouse wild-type AhR (mouse AhR Wt); (B) the mouse AhR with the triple substitutions I324M, A349T, and L363F (mouse 3mut); (C) the rabbit wild-type AhR (rabbit AhR Wt); and (D) the rabbit AhR with the triple substitutions M328I, T353A, and F367L (rabbit 3mut). Open circles represent 1, 10, 25, 50, and 100 μM OME; solid diamonds represent 0.01, 0.1, 0.3, 1, 3, 10, and 20 nM TCDD; open triangles represent 1, 10, 30, 100, 200, and 1000 nM 3MC; and solid squares with dotted lines represent 1, 10, 100, 300, 1000, and 2000 nM β-NF. Data represent the means of normalized firefly luciferase (FFluc)/*Renilla* luciferase activities from two independent experiments. EC_{50} values were calculated and are summarized in Table 1.

effective alternative to the phenylalanine required for reconstituting the response to OME in the mouse AhR (Fig. 6). It is interesting that there are differences between Leu and Val despite their structural similarity. Ala at position 349 in the mouse AhR is also conserved in rat and hamster AhRs, which exhibit only a slight response to OME. In human and guinea pig AhRs, which are OME-sensitive, the corresponding amino acid at this position is threonine, identical to the rabbit AhR. Overall, these three amino acid residues correspond strongly to the species differences in the response to OME. The differences in intensity of the response to OME among the animal species can be explained well by this comparative approach.

The results of our study suggest some possibilities for elucidating the underlying mechanism of OME-mediated AhR activation. In our experiments, the response required an OME-sensitive AhR that depended on three amino acid residues located in LBD. Some reports have suggested that PTK is associated with OME-mediated AhR activation (Kikuchi et al., 1998; Backlund and Ingelman-Sundberg, 2005). In one report, the Y320 residue of the human AhR was determined to be a putative phosphorylation site required for OME responsiveness (Lemaire et al., 2004). However, this tyrosine residue and the proximal nine amino acids are conserved in all the AhRs tested in the present study. Furthermore, the three amino acid residues that we found to be essential are not putative phosphorylation sites, nor are they included in the PTK consensus. Hence, AhR phosphorylation by PTK may be influenced by a conformational change resulting from these three amino acids. The mutant AhRs generated in the present study will be useful for further investigations of the relationship between OME and PTK. Other than the involvement of PTK, a possible mechanism for OME-mediated AhR activation is the presence of some type of ligand. A possible type of ligand is an endogenous (intrinsic) ligand in the culture medium or one that is generated intracellularly. In general, an endogenous ligand is considered to be inactivated rapidly by P450 enzymes (Chang and Puga, 1998; Adachi et al., 2001; Spink et al., 2003). In the presence of a P450 inhibitor, the endogenous ligand remains and may activate the AhR. In fact, the inhibitory effects of OME on CYP1A1, 2C19, and 3A4 have been reported previously (Li et al., 2004; Shiizaki et al., 2008). By disrupting an autoregulatory loop consisting of CYP1A1 and FICZ, one of the endogenous ligands, a recent report showed that CYP1A1 upregulation by CYP1A1-inhibiting chemicals was due to an indirect mechanism (Wincent et al., 2012). On the basis of this finding, we confirmed CYP1A1 inhibition by OME (Fig. 1) and demonstrated that CYP1A1 activity was required for OME-mediated AhR activation (Fig. 2). These results were quite similar to the results obtained from CYP1A1 inhibitor

TABLE 1
Summary of EC_{50} values of endogenous and synthetic chemical ligands

	Mouse (wt)	Mouse (3mt)[a]	Rabbit (wt)	Rabbit (3mt)[b]
Omeprazole (μM)	NR	17.4	19.2	NR
TCDD (nM)	2.05	1.97	1.98	1.25
3MC (nM)	18.2	12.5	47.5	76.2
β-NF (nM)	167	188	218	272
FICZ (nM)	3.34	5.26	18.8	24.0
Kynurenic acid (μM)	8.74	9.73	13.1	12.8
ITE (nM)	30.5	38.4	19.9	36.7
Indirubin (nM)	358	187	131	138

β-NF, β-naphthoflavone; NR, no response observed; wt, wild-type.
[a]Mouse (3mt): mouse AhR containing I324M, A349T, and L363F substitutions.
[b]Rabbit (3mt): rabbit AhR containing M328I, T353A, and F367L substitutions.

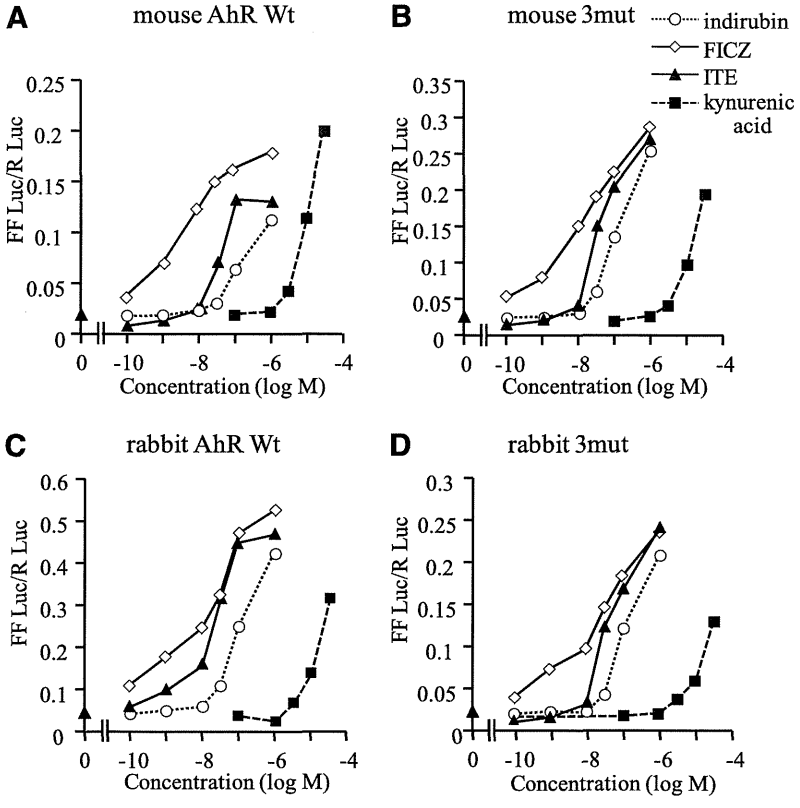

Fig. 11. Response of mouse and rabbit AhR mutants to known endogenous ligands: indirubin, FICZ, ITE, and kynurenic acid. HeLa cells were transfected with reporter genes and various AhRs: (A) the mouse wild-typeAhR (Mouse AhR Wt); (B) the mouse AhR with the triple substitutions I324M, A349T, and L363F (mouse 3mut); (C) the wild-type rabbit AhR (rabbit AhR Wt); and (D) rabbit AhR with the triple substitutions M328I, T353A, and F367L (rabbit 3mut). Open circles represent 0.1, 1, 10, 30, 100, and 1000 nM indirubin; open diamonds represent 0.1, 1, 10, 30, 100, and 1000 nM FICZ; solid triangles represent 0.1, 1, 10, 30, 100, and 1000 nM ITE; and solid squares represent 0.1, 1, 3, 10, and 30 μM kynurenic acid. Data represent the means of normalized firefly luciferase (FFluc)/*Renilla* luciferase activities from two independent experiments. EC_{50} values were calculated and are summarized in Table 1.

ellipticine. Furthermore, OME-mediated AhR activation was partially reduced as a result of charcoal-stripping of serum, which is considered to be a supplier of endogenous ligands (Fig. 3). Thus, we tested four putative endogenous ligands, including FICZ; however, AhR activation by these ligands was not significantly influenced by the three amino acid substitutions. We concluded that these four putative endogenous ligands are not involved in the indirect mechanism of OME-mediated AhR activation. Therefore, an enigmatic ligand may be involved. The possible mechanism related to the indirect activation of AhR by OME is illustrated in Supplemental Fig. 3. Another possible ligand is an unstable and short-lived metabolite of OME, which would be difficult to detect by general experimental procedures. Hu et al. developed a sensitive assay that indicated that OME itself could bind to AhR, although with a very low affinity (Hu et al., 2007). The results shown in Fig. 2 involve the possibility that CYP1A1 produces the putative active metabolite, and we do not have data that deny this hypothesis at present. If some ligand is related to OME-mediated AhR activation, it must differ in its affinity for rabbit and mouse AhRs, and the difference would be attributable to the three amino acid residues identified in this study.

In conclusion, three amino acids in the LBD of AhR define species-specific differences in OME-mediated AhR activation. These findings will be useful for elucidating the molecular mechanism underlying OME-mediated AhR activation.

Acknowledgments

The authors thank Dr. Kazuhiro Sogawa (Tohoku University, Japan) for providing the reporter plasmid pX4TK-Luc and Dr. Tomonari Matsuda (Kyoto University, Japan) for providing indirubin.

Authorship Contributions

Participated in research design: Shiizaki, Ohsako.

Conducted experiments: Shiizaki, Ohsako.

Contributed new reagents or analytic tools: Shiizaki, Ohsako, Kawanishi, Yagi.

Performed data analysis: Shiizaki.

Wrote or contributed to the writing of the manuscript: Shiizaki, Ohsako, Yagi.

References

Adachi J, Mori Y, Matsui S, Takigami H, Fujino J, Kitagawa H, Miller CA, 3rd, Kato T, Saeki K, and Matsuda T (2001) Indirubin and indigo are potent aryl hydrocarbon receptor ligands present in human urine. *J Biol Chem* **276**:31475–31478.

Backlund M and Ingelman-Sundberg M (2004) Different structural requirements of the ligand binding domain of the aryl hydrocarbon receptor for high- and low-affinity ligand binding and receptor activation. *Mol Pharmacol* **65**:416–425.

Backlund M and Ingelman-Sundberg M (2005) Regulation of aryl hydrocarbon receptor signal transduction by protein tyrosine kinases. *Cell Signal* **17**:39–48.

Backlund M, Johansson I, Mkrtchian S, and Ingelman-Sundberg M (1997) Signal transduction-mediated activation of the aryl hydrocarbon receptor in rat hepatoma H4IIE cells. *J Biol Chem* **272**:31755–31763.

Bohonowych JE and Denison MS (2007) Persistent binding of ligands to the aryl hydrocarbon receptor. *Toxicol Sci* **98**:99–109.

Burbach KM, Poland A, and Bradfield CA (1992) Cloning of the Ah-receptor cDNA reveals a distinctive ligand-activated transcription factor. *Proc Natl Acad Sci USA* **89**:8185–8189.

Chang CY and Puga A (1998) Constitutive activation of the aromatic hydrocarbon receptor. *Mol Cell Biol* **18**:525–535.

Curi-Pedrosa R, Daujat M, Pichard L, Ourlin JC, Clair P, Gervot L, Lesca P, Domergue J, Joyeux H, and Fourtanier G, et al. (1994) Omeprazole and lansoprazole are mixed inducers of CYP1A and CYP3A in human hepatocytes in primary culture. *J Pharmacol Exp Ther* **269**:384–392.

Daujat M, Peryt B, Lesca P, Fourtanier G, Domergue J, and Maurel P (1992) Omeprazole, an inducer of human CYP1A1 and 1A2, is not a ligand for the Ah receptor. *Biochem Biophys Res Commun* **188**:820–825.

Denison MS, Fisher JM, and Whitlock JP, Jr (1989) Protein-DNA interactions at recognition sites for the dioxin-Ah receptor complex. *J Biol Chem* **264**: 16478–16482.

Diaz D, Fabre I, Daujat M, Saint Aubert B, Bories P, Michel H, and Maurel P (1990) Omeprazole is an aryl hydrocarbon-like inducer of human hepatic cytochrome P450. *Gastroenterology* **99**:737–747.

DiNatale BC, Murray IA, Schroeder JC, Flaveny CA, Lahoti TS, Laurenzana EM, Omiecinski CJ, and Perdew GH (2010) Kynurenic acid is a potent endogenous aryl

hydrocarbon receptor ligand that synergistically induces interleukin-6 in the presence of inflammatory signaling. *Toxicol Sci* **115**:89–97.
Dzeletovic N, McGuire J, Daujat M, Tholander J, Ema M, Fujii-Kuriyama Y, Bergman J, Maurel P, and Poellinger L (1997) Regulation of dioxin receptor function by omeprazole. *J Biol Chem* **272**:12705–12713.
Ema M, Ohe N, Suzuki M, Mimura J, Sogawa K, Ikawa S, and Fujii-Kuriyama Y (1994) Dioxin binding activities of polymorphic forms of mouse and human arylhydrocarbon receptors. *J Biol Chem* **269**:27337–27343.
Fukunaga BN, Probst MR, Reisz-Porszasz S, and Hankinson O (1995) Identification of functional domains of the aryl hydrocarbon receptor. *J Biol Chem* **270**: 29270–29278.
Goryo K, Suzuki A, Del Carpio CA, Siizaki K, Kuriyama E, Mikami Y, Kinoshita K, Yasumoto K, Rannug A, and Miyamoto A, et al. (2007) Identification of amino acid residues in the Ah receptor involved in ligand binding. *Biochem Biophys Res Commun* **354**:396–402.
Hu W, Sorrentino C, Denison MS, Kolaja K, and Fielden MR (2007) Induction of cyp1a1 is a nonspecific biomarker of aryl hydrocarbon receptor activation: results of large scale screening of pharmaceuticals and toxicants in vivo and in vitro. *Mol Pharmacol* **71**:1475–1486.
Karchner SI, Franks DG, Kennedy SW, and Hahn ME (2006) The molecular basis for differential dioxin sensitivity in birds: role of the aryl hydrocarbon receptor. *Proc Natl Acad Sci USA* **103**:6252–6257.
Kennedy SW and Jones SP (1994) Simultaneous measurement of cytochrome P4501A catalytic activity and total protein concentration with a fluorescence plate reader. *Anal Biochem* **222**:217–223.
Kikuchi H, Fukushige S, Shibazaki M, and Shiratori Y (2002) Presence on human chromosome 10 of omeprazole-sensitivity gene whose product mediates CYP1A1 induction. *Cytogenet Genome Res* **97**:51–57.
Kikuchi H, Hossain A, Sagami I, Ikawa S, and Watanabe M (1995) Different inducibility of cytochrome P-4501A1 mRNA of human and mouse by omeprazole in culture cells. *Arch Biochem Biophys* **316**:649–652.
Kikuchi H, Hossain A, Yoshida H, and Kobayashi S (1998) Induction of cytochrome P-450 1A1 by omeprazole in human HepG2 cells is protein tyrosine kinase-dependent and is not inhibited by alpha-naphthoflavone. *Arch Biochem Biophys* **358**:351–358.
Kimura A, Naka T, Nohara K, Fujii-Kuriyama Y, and Kishimoto T (2008) Aryl hydrocarbon receptor regulates Stat1 activation and participates in the development of Th17 cells. *Proc Natl Acad Sci USA* **105**:9721–9726.
Krusekopf S, Kleeberg U, Hildebrandt AG, and Ruckpaul K (1997) Effects of benzimidazole derivatives on cytochrome P450 1A1 expression in a human hepatoma cell line. *Xenobiotica* **27**:1–9.
Lemaire G, Delescluse C, Pralavorio M, Ledirac N, Lesca P, and Rahmani R (2004) The role of protein tyrosine kinases in CYP1A1 induction by omeprazole and thiabendazole in rat hepatocytes. *Life Sci* **74**:2265–2278.
Li XQ, Andersson TB, Ahlström M, and Weidolf L (2004) Comparison of inhibitory effects of the proton pump-inhibiting drugs omeprazole, esomeprazole, lansoprazole, pantoprazole, and rabeprazole on human cytochrome P450 activities. *Drug Metab Dispos* **32**:821–827.
Lind T, Cederberg C, Ekenved G, Haglund U, and Olbe L (1983) Effect of omeprazole—a gastric proton pump inhibitor—on pentagastrin stimulated acid secretion in man. *Gut* **24**:270–276.
Mimura J, Ema M, Sogawa K, and Fujii-Kuriyama Y (1999) Identification of a novel mechanism of regulation of Ah (dioxin) receptor function. *Genes Dev* **13**:20–25.
Murray IA, Morales JL, Flaveny CA, Dinatale BC, Chiaro C, Gowdahalli K, Amin S, and Perdew GH (2010) Evidence for ligand-mediated selective modulation of aryl hydrocarbon receptor activity. *Mol Pharmacol* **77**:247–254.
Murray IA, Reen RK, Leathery N, Ramadoss P, Bonati L, Gonzalez FJ, Peters JM, and Perdew GH (2005) Evidence that ligand binding is a key determinant of Ah receptor-mediated transcriptional activity. *Arch Biochem Biophys* **442**:59–71.
Pollenz RS, Sattler CA, and Poland A (1994) The aryl hydrocarbon receptor and aryl hydrocarbon receptor nuclear translocator protein show distinct subcellular localizations in Hepa 1c1c7 cells by immunofluorescence microscopy. *Mol Pharmacol* **45**:428–438.
Quattrochi LC and Tukey RH (1993) Nuclear uptake of the Ah (dioxin) receptor in response to omeprazole: transcriptional activation of the human CYP1A1 gene. *Mol Pharmacol* **43**:504–508.
Quintana FJ, Basso AS, Iglesias AH, Korn T, Farez MF, Bettelli E, Caccamo M, Oukka M, and Weiner HL (2008) Control of $T_{(reg)}$ and $T_{(H)}17$ cell differentiation by the aryl hydrocarbon receptor. *Nature* **453**:65–71.
Reyes H, Reisz-Porszasz S, and Hankinson O (1992) Identification of the Ah receptor nuclear translocator protein (Arnt) as a component of the DNA binding form of the Ah receptor. *Science* **256**:1193–1195.
Shiizaki K, Ohsako S, Kawanishi M, and Yagi T (2008) Omeprazole alleviates benzo [a]pyrene cytotoxicity by inhibition of CYP1A1 activity in human and mouse hepatoma cells. *Basic Clin Pharmacol Toxicol* **103**:468–475.
Shiizaki K, Ohsako S, Koyama T, Nagata R, Yonemoto J, and Tohyama C (2005) Lack of CYP1A1 expression is involved in unresponsiveness of the human hepatoma cell line SK-HEP-1 to dioxin. *Toxicol Lett* **160**:22–33.
Song J, Clagett-Dame M, Peterson RE, Hahn ME, Westler WM, Sicinski RR, and DeLuca HF (2002) A ligand for the aryl hydrocarbon receptor isolated from lung. *Proc Natl Acad Sci USA* **99**:14694–14699.
Spink BC, Hussain MM, Katz BH, Eisele L, and Spink DC (2003) Transient induction of cytochromes P450 1A1 and 1B1 in MCF-7 human breast cancer cells by indirubin. *Biochem Pharmacol* **66**:2313–2321.
Wei YD, Helleberg H, Rannug U, and Rannug A (1998) Rapid and transient induction of CYP1A1 gene expression in human cells by the tryptophan photoproduct 6-formylindolo[3,2-b]carbazole. *Chem Biol Interact* **110**:39–55.
Wincent E, Bengtsson J, Mohammadi Bardbori A, Alsberg T, Luecke S, Rannug U, and Rannug A (2012) Inhibition of cytochrome P4501-dependent clearance of the endogenous agonist FICZ as a mechanism for activation of the aryl hydrocarbon receptor. *Proc Natl Acad Sci USA* **109**:4479–4484.
Yoshinari K, Ueda R, Kusano K, Yoshimura T, Nagata K, and Yamazoe Y (2008) Omeprazole transactivates human CYP1A1 and CYP1A2 expression through the common regulatory region containing multiple xenobiotic-responsive elements. *Biochem Pharmacol* **76**:139–145.

Address correspondence to: Takashi Yagi, Department of Biology, Graduate School of Science, Osaka Prefecture University, 1-2 Gakuen-cho, Naka-ku, Sakai, Osaka, Japan. E-mail: yagi-t@riast.osakafu-u.ac.jp

Acta Histochemica 116 (2014) 474–480

Contents lists available at ScienceDirect

Acta Histochemica

journal homepage: www.elsevier.de/acthis

Single administration of butylparaben induces spermatogenic cell apoptosis in prepubertal rats

Mohammad Shah Alam[a,b], Seiichiroh Ohsako[c], Yoshiakira Kanai[b], Masamichi Kurohmaru[b,*]

[a] Department of Anatomy and Histology, Faculty of Veterinary Medicine and Animal, Science, Bangabandhu Sheikh Mujibur Rahman Agricultural University, Gazipur 1706, Bangladesh
[b] Department of Veterinary Anatomy, Graduate School of Agricultural and Life Sciences, The University of Tokyo, 1-1-1 Yayoi, Bunkyo-ku, Tokyo 113-8657, Japan
[c] Laboratory of Environmental Health Sciences, Center for Disease Biology and Integrative Medicine, Graduate School and Faculty of Medicine, The University of Tokyo, 7-3-1 Hongo, Bunkyo-Ku, Tokyo 113-0033, Japan

ARTICLE INFO

Article history:
Received 30 August 2013
Received in revised form 5 October 2013
Accepted 6 October 2013

Keywords:
Butylparaben
Prepubertal stage
Spermatogenic cell apoptosis
Rat

ABSTRACT

Parabens are *p*-hydroxybenzoic acid ester compounds widely used as preservatives in foods, cosmetics, toiletries and pharmaceuticals. Some parabens, including butylparaben, exert an estrogenic activity as determined by *in vitro* estrogen receptor assay and *in vivo* uterotrophic assay, and adversely affect endocrine secretion and male reproductive function. We conducted a research study to evaluate the acute effects of butylparaben on testicular tissues of prepubertal rats. Three-week-old male rats ($n=8$) were given a single dose of 1000 mg/kg butylparaben. The rats were sacrificed under anesthesia at 3, 6 and 24 h after administration, and their testes were collected for histopathological examination. The study revealed progressive detachment and sloughing of spermatogenic cells into the lumen of the seminiferous tubules at 3 h, and this effect was enhanced at 6 h after administration. Thin seminiferous epithelia and wide tubular lumina were seen at 24 h in the butylparaben-treated group, compared to the control. In order to clarify whether sloughed spermatogenic cells underwent apoptosis, TUNEL assay was carried out. We found a significant increase in the number of apoptotic spermatogenic cells in all the treated groups, compared to the controls and a maximal number of apoptotic cells were detected at 6 h after administration. In semithin sections, apoptotic cells were easily detected by their prominent basophilia and condensed chromatin, mainly found in spermatocytes. Ultrastructurally, the condensed chromatin and shrunken cytoplasm and nucleus, hallmarks of apoptotic cell death, were observed in butylparaben-treated groups. These observations lead us to postulate that butylparaben, similar to other estrogenic compounds, also induces spermatogenic cell apoptosis.

Introduction

Parabens are a group of alkyl esters of *p*-hydroxybenzoic acid and typically include methylparaben, ethylparaben, propylparaben, butylparaben, isobutylparaben, isopropylparaben, and benzylparaben. Humans are exposed to these parabens *via* personal care products, owing to their extensive use in cosmetics, toiletries, food, and pharmaceuticals. Upon dietary exposure, parabens are rapidly hydrolyzed in the gut by esterases to different metabolites (Derache and Gourdon, 1963). In several *in vitro* studies, parabens were able to bind to estrogen receptors (ERs), activating genes controlled by hormones *via* the receptor (Byford et al., 2002; Pugazhendhi et al., 2005; Prusakiewicz et al., 2007). Administration of butylparaben has also been shown to increase uterine weight *in vivo* in both immature rats and mice and in adult ovariectomized mice, hence confirming its estrogenic activity (Soni et al., 2005; Routledge et al., 1998).

Prepubertal mice (4-weeks-old) treated with butylparaben for 10 weeks showed a dose-dependent decrease of both round and elongated spermatid counts and serum testosterone levels in all the treated groups (Oishi, 2002). It was further demonstrated (Oishi, 2004) that decreased testicular testosterone levels caused alterations of male reproductive function in prepubertal rats after propylparaben administration for 7 days. Nevertheless, it was also shown that neither male reproductive functions nor serum hormone levels including testosterone, LH and FSH were affected by methylparaben and ethylparaben at a dose of about 1000 mg/kg/day (Oishi, 2004).

* Corresponding author.
E-mail address: amkuroh@mail.ecc.u-tokyo.ac.jp (M. Kurohmaru).

0065-1281/$ – see front matter © 2013 Published by Elsevier GmbH.
http://dx.doi.org/10.1016/j.acthis.2013.10.006

It has been reported that *in utero* exposure of butylparaben decreased steroidogenesis by interfering with the transport of cholesterol to mitochondria (Taxvig et al., 2008). In another study (Song et al., 1991) showed that butylparaben exerts an inhibitory effect on the acrosomal enzyme acrosin, and impairs sperm membrane function, suggesting that spermatogenic cells could be a target of parabens in the testis (Tavares et al., 2009). As far as we are aware there are no published reports regarding spermatogenic cell apoptotic index induced by parabens.

It has been demonstrated that several environmental endocrine disruptors have activities similar to those of endogenous estrogen (17β-estradiol) or antiandrogens, including bisphenol A (vom Saal et al., 1998), alkylphenol (Routledge and Sumpter, 1997) and phthalates (Alam et al., 2010b). These estrogenic compounds can cause alterations in circulating concentrations of gonadotropins (LH, FSH) and testicular testosterone, and thus can interfere with spermatogenesis. In previous studies in prepubertal rats we demonstrated that a single dose of estrogenic compounds, such as di(*n*-butyl) phthalate and estradial-3-benzoate, inhibits testicular steroidogenesis and decreases serum LH and FSH levels, together with significantly increasing spermatogenic cell apoptosis (Alam et al., 2010b). Many of the parabens, including butylparaben, are thought to possess estrogenic activity leading to reduced testosterone levels and lower counts of both round and elongated spermatids (Routledge et al., 1998; Pedersen et al., 2000; Okubo et al., 2001; Byford et al., 2002; Oishi, 2002; Taxvig et al., 2008). In the present study, we investigated histochemically the possible acute effects of butylparaben on testes at prepubertal stage on apoptotic inducibility, which is a specific feature of estrogenic compounds.

Materials and methods

Chemicals

Butylparaben (purity > 99% purity) was purchased from Wako Pure Chemical Industries (Osaka, Japan). Proteinase K and 3,3′-diaminobenzidine tetrahydrochloride (DAB) were from TaKaRa (Otsu, Japan). Neutral buffered formalin and propylene oxide were from Wako. Osmium tetroxide and Araldite M were from Nisshin EM Co. (Tokyo, Japan). The terminal deoxy-nucleotidyl transferase-mediated digoxigenin-dUTP nick-end labeling (TUNEL) (*In Situ* Apoptotic Detection) Kit was purchased from TaKaRa.

Animals and treatments

Male Sprague-Dawley rats (3-weeks-old) were purchased from Charles River Laboratories (Tokyo, Japan). The rats were housed three to five per plastic cage, maintained on a 12 h light/dark cycle at a constant temperature (22 °C ± 1 °C) and humidity (45–70%), and provided water and rodent pellets (Oriental Yeast, Tokyo, Japan) *ad libitum*. Animals were maintained and handled humanely in accordance with the guidelines on animal experiments of the Institutional Animal Care and Use Committee (IACUC) of the University of Tokyo, Tokyo, Japan. Three-week-old male rats ($n = 8$) were given a single oral administration of 1000 mg/kg butyloraben in vehicle at a volume equal to 4 ml/kg. The vehicle was a mixture of 5% ethanol and 95% corn oil. Control animals received the same volume of vehicle. Rats were then killed under diethyl ether anesthesia at 3, 6 and 24 h after administration, and their testes were collected and subjected to histopathology.

Light microscopy

For histopathological observations (hematoxylin and eosin, TUNEL), under diethyl ether anesthesia, rats were perfused with 10% neutral buffered formalin for 30 min. Following perfusion, the testes were excised and immersed in the same fixative for 48 h. Then, the samples were washed in 0.1 M phosphate buffer solution for 3 h, dehydrated through a graded series of ethanol, cleared in xylene, and embedded in paraffin. Sections from the paraffin blocks were cut at 4 μm in thickness. The sections were then stained with Meyer's hematoxylin and eosin (H&E) and/or periodic acid-Schiff (PAS)-hematoxylin (Wako, Osaka, Japan). The samples were studied with an Olympus (BX50) light microscope (Tokyo, Japan).

TUNEL assay

In order to quantitatively assess the incidence of apoptotic spermatogenic cells after treatment, *in situ* terminal deoxynucleotidyl transferase-mediated digoxigenin-dUTP nick-end-labeling (TUNEL) assay was performed using an Apoptotic Detection Kit according to the manufacturer's instructions. Briefly, the testes sections were deparaffinized and digested with 10 μg/ml proteinase K at 37 °C for 15 min. After being washed three to five times with 0.01 M phosphate buffer solution (PBS, pH7.4), they were treated with terminal deoxynucleotidyl transferase (TdT) enzyme and Labeling Safe Buffer, which were included in the kit. The TdT reaction was conducted at 37 °C for 90 min. To check for the non-specific reaction, the sections were incubated with PBS alone instead of FITC-labeled TdT enzyme. After further washing three to five times with PBS, they were incubated with horseradish peroxidase (HRP) goat anti-biotin at 37 °C for 30 min. The localization of HRP sites was determined by application of DAB. The sections were then counterstained with methyl green and mounted. Images of seminiferous tubules were obtained by using an Olympus (BX50) light microscope connected to a digital camera (DP20, Olympus, Tokyo, Japan). Using a ×20 objective, 3 fields in each section were randomly selected. The area of seminiferous tubules in all fields was measured by a computer assisted system using Scion Image software (Scion Co., Frederick, MD, USA). Then, TUNEL-positive (brown-stained) spermatogenic cells in all selected areas were counted. The number of TUNEL-positive cells per 1 mm^2 seminiferous tubule was calculated as described in our previous study (Alam et al., 2010b). Data were obtained from 4 rats in each group and were given as mean ± S.E.M.

Transmission electron microscopy

For transmission electron microscopy, under diethyl ether anesthesia, rats were perfused with 5% glutaraldehyde in 0.1 M phosphate buffer, and then the testes were excised, immersed in the same fixative at 4 °C for 3 h and postfixed in 1% osmium tetroxide (OsO_4) at 4 °C for 2 h. The samples were then dehydrated in ethanol, infiltrated in propylene oxide, and embedded in Araldite M. Semi-thin sections were cut at 1 μm in thickness, stained with 1% toluidine blue, and observed by light microscopy. Ultrathin sections were cut, and stained with uranyl acetate and lead citrate. In the butylparaben-treated rats, unique lesions were encountered at the light microscopic level at 24 h. Corresponding tissue sections from these animals, along with appropriate control sections, were examined using a JEM-1010 transmission electron microscope at 80 kV (JEOL, Tokyo, Japan). Evaluation was limited to characterization of subtle lesions and abnormal cells, because quantitative analysis is very limited with electron microscopy.

Statistical analysis

Statistical analysis was performed using Stat View software (SAS Institute Inc., Cary, NC, USA). All results are represented as the means ± S.E.M. For the comparison of apoptotic spermatogenic cell index, one-way analysis of variance (ANOVA) was carried out followed by Fisher's PLSD as a *post hoc* test. Differences were

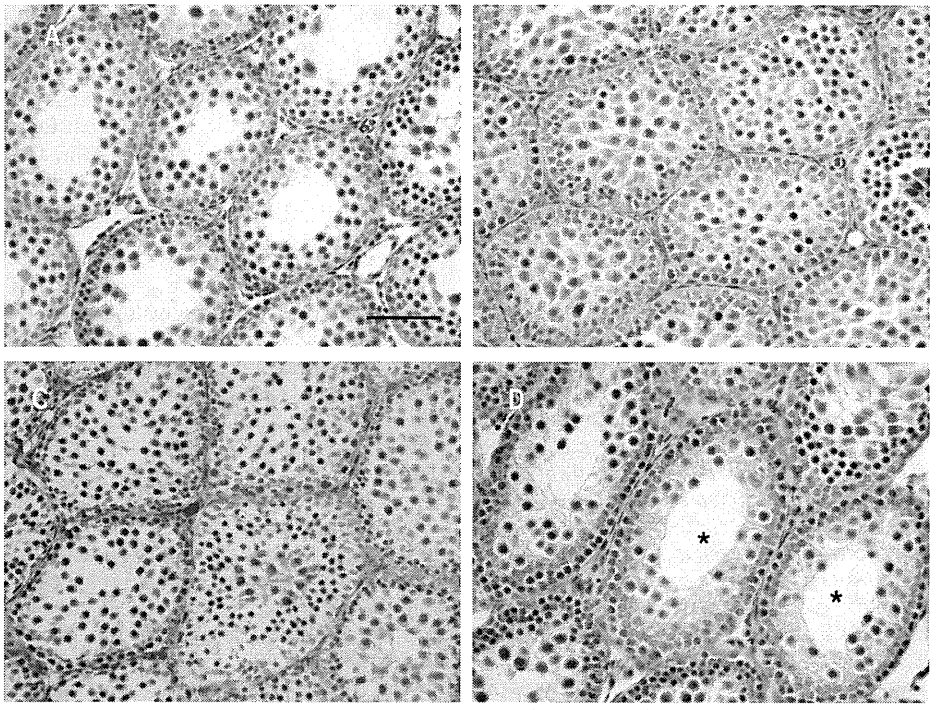

Fig. 1. Histopathological changes in testes after single administration of 1000 mg/kg butylparaben are shown. Control of vehicle administration at 24 h (A). Reduction of tubular lumen due to detachment and displacement of spermatogenic cells at 3 h after administration (B), Sloughing of spermatogenic cells at 6 h (C). Thin seminiferous epithelia and wide tubular lumen (*) at 24 h (D). Scale bar = 50 μm.

considered to be statistically significant when the *P* value was less than 0.05.

Results

Histopathology

Histopathology was evaluated using cross-sections of seminiferous tubules stained with hematoxylin and eosin by light microscopy. Due to progressive detachment and sloughing of spermatogenic cells into the lumen of the seminiferous tubules, reduction and/or disappearance of tubular lumen was observed at 3 h after butylparaben treatment (Fig. 1B). This effect was enhanced at 6 h since Sertoli cells and spermatogonia with few spermatocytes remained within the seminiferous tubules (Fig. 1C). Thin seminiferous epithelia and wide tubular lumen were recognized at 24 h (Fig. 1D) after butylparaben treatment, compared to the vehicle treated control at 24 h (Fig. 1A). Since in all time schedules, the vehicle-treated control had the same manner of seminiferous epithelia structure, the longest period (24 h) of vehicle treated group was chosen for the control (Fig. 1A).

Apoptosis

We carried out a TUNEL assay to detect whether sloughed spermatogenic cells were undergoing apoptosis. We found a significant increase in the number of apoptotic spermatogenic cells in the treated groups in comparison with the control group (Fig. 2). The maximal number of apoptotic spermatogenic cells was detected at 6 h after treatment (Fig. 2C and E). At 24 h after administration, the number of apoptotic cells began to gradually decline, though it was still significantly greater than that in the control group (Fig. 2D and E). In order to evaluate the spermatogenic cell types that underwent apoptosis, apoptotic cells were analyzed by light microscopy (semithin sections) and transmission electron microscopy. In semithin sections stained with toluidine blue, degenerative spermatogenic cells were easily detected by their prominent basophilia, condensed nuclear chromatin and shrinkage of cytoplasm (Fig. 3A–D). Apoptotic spermatogenic cells were frequently observed in the butylparaben-treated group, compared with the control group (Fig. 3). Close observations showed the apoptotic (nuclear chromatin condensed) cells were rounded-up and surrounded by an empty space. They might separate from their neighbors. Spermatocytes were the largest cells and showed typically dispersed chromatin, and spermatogonia were identified by their location (within the basal compartment, among the Sertoli cells). Similarly, at the transmission electron microscopic level, the condensed chromatin and shrinkage of cytoplasm and nucleus were observed. The apoptotic spermatocytes might be phagocytosed by neighboring Sertoli cells (Fig. 3F). These data indicate that butylparaben induces apoptotic cell death in testes and is most commonly found in spermatocytes, less frequently in spermatids, and not in spermatogonia and somatic cells (Sertoli cells or Leydig cells).

Discussion

We used prepubertal rats in the present study and observed the testicular alterations after a single administration of butylparaben. The prepubertal stage is much more sensitive than adults (Kondo et al., 2006), and rats are more sensitive to endocrine disruptors than mice. A massive number of spermatogenic cells undergo apoptosis in the first wave of spermatogenesis (first to seven weeks of postnatal life), and the highest rate of apoptosis occurs at 18–26 days of age to maintain an optimum Sertoli and spermatogenic cells ratio (Yan et al., 2000). Apoptosis is a process of cell death and is involved in various physiological and pathological events (Saikumar et al., 1999). During various stages of mammalian spermatogenesis, spermatogenic cell apoptosis occurs to remove abnormal spermatogenic cells and to maintain normal quantity and quality of sperm afterwards (Billig et al., 1995; Print and Loveland,

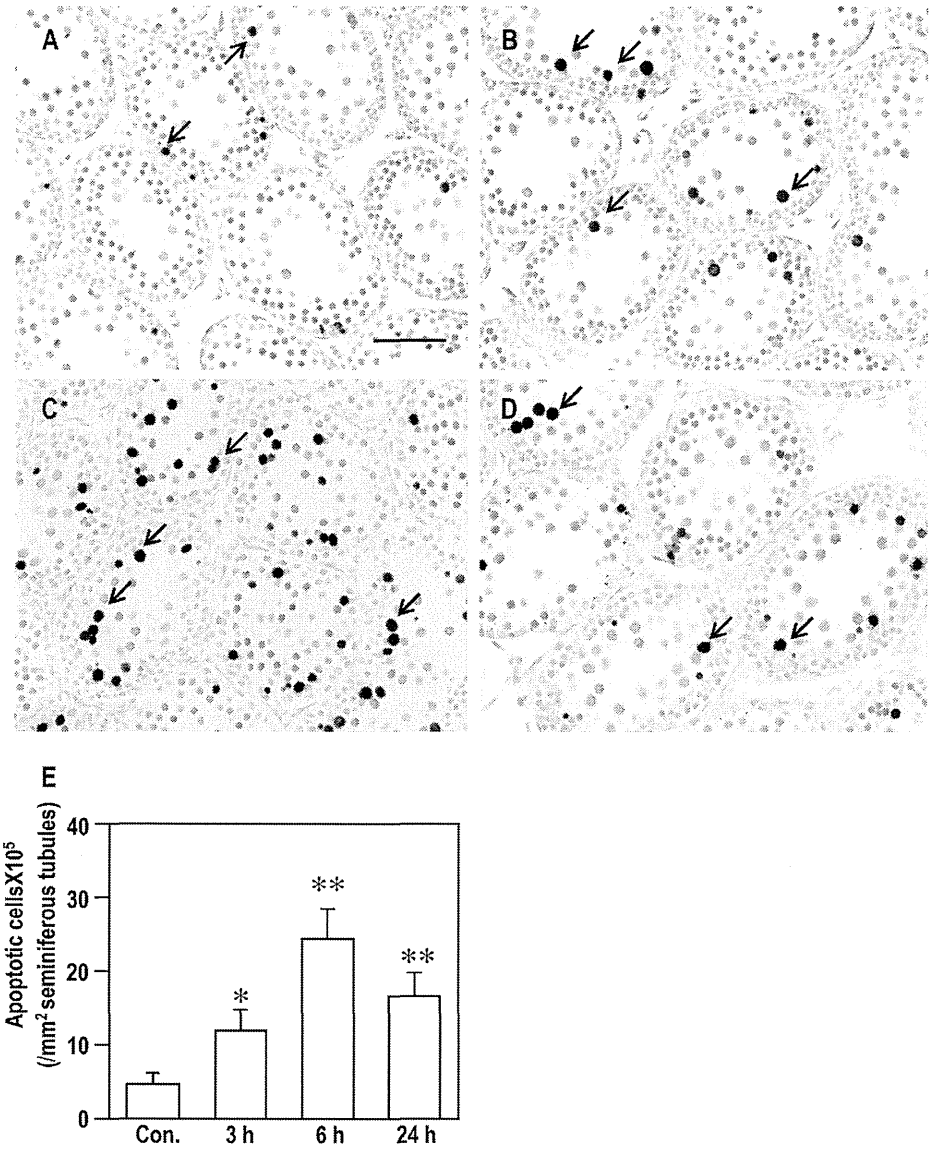

Fig. 2. TUNEL assay of testicular sections for apoptotic spermatogenic cells by single administration of butylparaben. Vehicle-treated control (A), and at 3 h (B), at 6 h (C), and at 24 h (D) after administration. Arrows indicate apoptotic cells. Note the maximal apoptotic cell number at 6 h after administration. Scale bar = 50 μm. Quantification of apoptotic cells (E). Values representing the number of apoptotic cells/mm^2 cross sectional area of seminiferous tubules are expressed as the eans ± SE (n = 8). Statistically significant differences between means from the control and treated groups were determined by ANOVA followed by Fisher's PLSD test (*P < 0.05; ** P < 0.01, *versus* control).

2000). Spermatogenic cell apoptosis is also induced by many factors including hormonal deprivation, heat, radiation and environmental endocrine disruptors (Koji and Hishikawa, 2003; Shaha, 2007). Excessive and/or abnormal apoptosis of spermatogenic cells is one of the main reasons for oligozoospermia and azoospermia (Tesarik et al., 1998).

There is much evidence that butylparaben can interact with estrogen receptors (ERs). For example, several studies employing an ER-mediated yeast growth assay or a reporter assay with human breast cancer cell line MCF-7 have demonstrated the interaction between butylparaben and ERs (Routledge et al., 1998; Pedersen et al., 2000; Okubo et al., 2001). Routledge et al. (1998) reported that estrogenic activity was inhibited by 4-hydroxy tamoxifen. In addition, proliferative effects of parabens on MCF-7 cells were completely suppressed by the anti-estrogen ICI 182,780 *in vitro* (Okubo et al., 2001). Moreover, butylparaben has also been shown to increase uterine weight in both immature rats and mice and in adult ovariectomized mice in the rat uterotrophic assay (Routledge et al., 1998), thus indicating its estrogenic activity. Decreased testicular testosterone biosynthesis, as well as decreased serum LH and serum FSH levels, occurs after exogenous estrogen exposure, together with increased spermatogenic cell apoptosis (D'Souza et al., 2005; Alam et al., 2010b). Similarly, butylparaben has been shown to decrease serum testosterone levels, resulting in decreased counts of round and elongated spermatids (Byford et al., 2002; Oishi, 2002; Taxvig et al., 2008). As far as we are aware, the present study has shown for the first time that butylparaben induces increased apoptosis of spermatogenic cell shortly after treatment. These findings agree well with our previous data on di(n-butyl) phthalate, a suspected estrogenic compound, which significantly increases spermatogenic cell apoptosis in prepubertal rats (Alam et al., 2010a,b). The mechanism how butylparaben induces spermatogenic cell apoptosis is not known at present and further exploration is needed. The development of the male reproductive system and

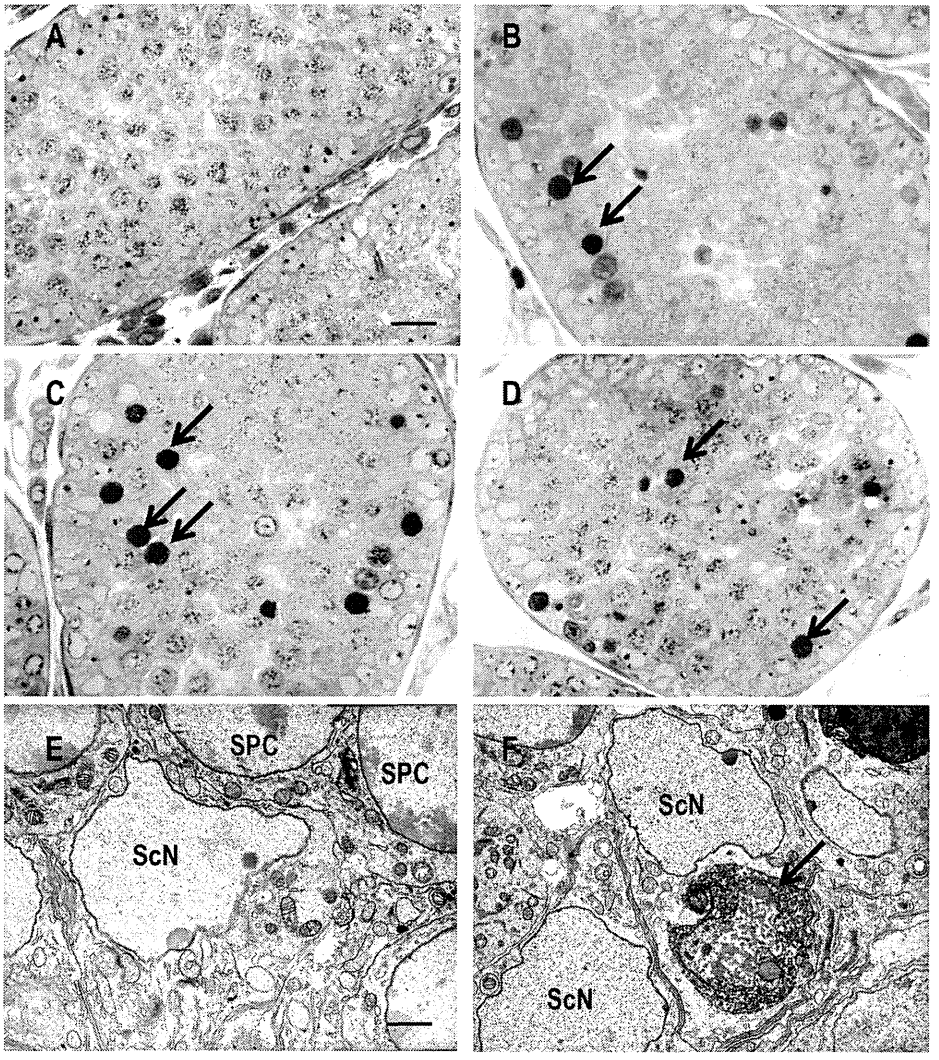

Fig. 3. Semithin sections (A–D) and transmission electron micrographs (E–F) of seminiferous tubules after single butylparaben administration. Vehicle-treated control (A), and at 3 h (B), at 6 h (C), and at 24 h (D) after treatment. Arrows indicate apoptotic spermatogenic cells. Scale bar = 20 μm. Control rats showing normal Sertoli cell nucleus (ScN), spermatogonium (SG), and spermatocyte (SPC) (E). An apoptotic spermatogenic cell characterized by heterochromatin condensation and shrinkage of cytoplasm surrounded by a normal Sertoli cell nucleus is distinctly observed at 24 h (F). Scale bar = 2 μm.

spermatogenesis are controlled by testosterone. Although the possibility that decreased testosterone levels may result in the increase in spermatogenic cell apoptosis cannot be ruled out, it seems to be due to direct cytotoxic effects of parabens on spermatogenic cells or estrogenic action. For example, our previous study has demonstrated that an estrogenic compound, such as di(*n*-butyl) phthalate/estradiol-3-benzoite-induced spermatogenic cell apoptosis was not associated with testicular steroidogenesis (Alam et al., 2010b).

It has also been reported that estrogen directly induces spermatogenic cell apoptosis by cytochrome c release from mitochondria and FasL up-regulation in *in vitro* model with isolated spermatogenic cells (Mishra and Shaha, 2005). However, this apoptosis was inhibited by tamoxifen, indicating that an estrogen-induced change occurs through hormone receptor interaction in spermatogenic cells. Therefore, it is possible to postulate that the ERs present in testes, probably in spermatocytes and spermatids, have a role in inducing spermatogenic cell apoptosis when binding to exogenous estrogenic compounds including butylparaben. Indeed, both ERα and ERβ are present in rat spermatocytes and round spermatids (Saunders et al., 1998; Pelletier et al., 2000). In the present study, we also observed that butylparaben-induced apoptosis was commonly found in spermatocytes, less frequently in spermatids and not found in spermatogonia and somatic cells. Moreover, butylparaben adversely affects spermatozoa by an inhibitory effect on acrosin and impairment of sperm membrane function (Song et al., 1991), suggesting that spermatogenic cells are a direct target of parabens in testicular toxicity (Tavares et al., 2009). In addition, our previous studies have reported that disruption of Sertoli cell-spermatogenic cell physical interactions leads to detachment and sloughing of spermatogenic cells from the seminiferous epithelium after exposure to phthalates, and these detached spermatogenic cells lost the support and nurture provided by Sertoli cells and eventually undergo apoptosis (Alam et al., 2010c). Similarly, in the present study, we also observed that apoptotic cells become detached from their neighbors, probably due to collapse of Sertoli cell vimentin filaments.

The maximal number of apoptotic spermatogenic cells was found at 6 h after butylparaben administration, and at 24 h, the number of apoptotic cells began to decline, though it was still significantly greater than that in the control group. This is most probably due to the rapid elimination of apoptotic cells by phagocytosis, a

common fate of cells undergoing apoptosis (Maeda et al., 2002; Tay et al., 2007). In the present finding, in transmission electron microscopy, apoptotic cells appeared to be engulfed by neighboring Sertoli cells. Sertoli cells play an important role in clearing apoptotic spermatogenic cells by the process of phagocytosis. It is likely to be a self-defense mechanism (Maeda et al., 2002). During spermatogenic cell differentiation, although more than half of differentiating spermatogenic cells die by apoptosis before they mature into spermatozoa (Dym, 1994), only a limited number of apoptotic cells are detected when testicular sections are examined by TUNEL assay (Koji et al., 2001; Maeda et al., 2002). Unfortunately, the role of phagocytosis in butylparaben administration cannot be ascertained at present, and further exploration is needed.

In conclusion, the present results of single butylparaben administration in prepubertal rats demonstrated histopathological changes in the seminiferous tubules and loss of spermatogenic cells by apoptosis. Because of the importance of these effects, more detailed studies on the mechanism of toxicity induced by parabens in the male reproductive organs are necessary. This study is now underway in our laboratory to elucidate the mechanism of action of testicular dysfunction induced by parabens.

Acknowledgments

We thank Dr. Andriana Bibin for his technical support during TEM handling in this study. This work was supported in part by Grants-in-Aid from the Ministry of Education, Science, and Culture, Japan.

References

Alam MS, Andriana BB, Tay TW, Tsunekawa N, Kanai Y, Kurohmaru M. Single administration of di(*n*-butyl) phthalate delays spermatogenesis in prepubertal rats. Tissue Cell 2010a;42:129–35.

Alam MS, Ohsako S, Matsuwaki T, Zhu XB, Tsunekawa N, Kanai Y, et al. Induction of spermatogenic cell apoptosis in prepubertal rat testes irrespective of testicular steroidogenesis: a possible estrogenic effects of di(*n*-butyl) phthalate. Reproduction 2010b;139:427–37.

Alam MS, Ohsako S, Tay TW, Tsunekawa N, Kanai Y, Kurohmaru M. Di(*n*-butyl) phthalate induces vimentin filaments disruption in rat Sertoli cells: a possible relation with spermatogenic cell apoptosis. Anat Histol Embryol 2010c;39:186–93.

Billig H, Furuta I, River C, Tapanainen J, Parvinen M, Hsueh AJ. Apoptosis in testis germ cells: developmental changes in gonadotropin dependence and localization to selective tubule stages. Toxicology 1995;1:189–95.

Byford JR, Shaw LE, Drew MG, Pope GS, Sauer MJ, Darbre PD. Oestrogenic activity of parabens in MCF7 human breast cancer cells. J Steroid Biochem Mol Biol 2002;80:49–60.

Derache R, Gourdon J. Metabolism of a food preservation: parahydroxybenzoic acid and its esters. Food Cosmetic Toxicol 1963;1:189–95.

D'Souza R, Gill-Sharma MK, Pathak S, Kedia N, Kumar R, Balasinor N. Effect of high intratesticular estrogen on the seminiferous epithelium in adult male rats. Mol Cell Endocrinol 2005;241:41–8.

Dym M. Spermatogonial stem cells of the testis. Proc Natl Acad Sci U S A 1994;91:11287–9.

Koji T, Hishikawa Y. Germ cell apoptosis and its molecular trigger in mouse testes. Arch Histol Cytol 2003;66:1–16.

Koji T, Hishikawa Y, Ando H, Nakanishi Y, Kobayashi N. Expression of Fas and Fas ligand in normal and ischemia-reperfusion testes: involvement of the Fas system in the induction of germ cell apoptosis in the damaged mouse testis. Biol Reprod 2001;64:946–54.

Kondo T, Shono T, Suita S. Age-specific effect of phthalate ester on testicular development in rats. J Pediatr Surg 2006;41:1290–3.

Maeda Y, Shiratsuchi A, Namiki M, Nakanishi Y. Inhibition of sperm production in mice by annexin V microinjected into seminiferous tubules: possible etiology of phagocytic clearance of apoptotic spermatogenic cells and male infertility. Cell Death Differ 2002;9:742–9.

Mishra DP, Shaha C. Estrogen-induced spermatogenic cell apoptosis occurs via the mitochondrial pathway: role of superoxide and nitric oxide. J Biol Chem 2005;280:96–6181.

Oishi S. Lack of spermatotoxic effects of methyl and ethyl esters of *p*-hydroxybenzoic acid in rats. Food Chem Toxicol 2004;42:54–1845.

Oishi S. Effects of butyl paraben on the male reproductive system in mice. Arch Toxicol 2002;76:423–9.

Okubo T, Yokoyama Y, Kano K, Kano I. ER-dependent oestrogenic activity of parabens assessed by proliferation of human breast cancer MCF-7 cells and expression of ERa and PR. Food Chem Toxicol 2001;39:32–1225.

Pedersen KL, Pedersen SN, Christiansen LB, Korsgaard B, Bjerregaard P. The preservatives ethyl-, propyl- and butyl paraben are estrogenic in an in vivo fish assay. Pharmacol Toxicol 2000;86:110–3.

Pelletier G, Labrie C, Labrie F. Localization of oestrogen receptor alpha, oestrogen receptor beta and androgen receptors in the rat reproductive organs. J Endocrinol 2000;165:359–70.

Print CG, Loveland KL. Germ cell suicide: new insights into apoptosis during spermatogenesis. BioEssays 2000;22:423–30.

Prusakiewicz JJ, Harville HM, Zhang Y, Ackermann C, Voorman RL. Parabens inhibit human skin estrogen sulfotransferase activity: possible link to paraben estrogenic effects. Toxicology 2007;232:248–56.

Pugazhendhi D, Pope GS, Darbre PD. Oestrogenic activity of p-hydroxybenzoic acid (common metabolite of paraben esters) and methylparaben in human breast cancer cell lines. J Appl Toxicol 2005;25:301–9.

Routledge EJ, Parker J, Odum J, Ashby J, Sumpter JP. Some alkyl hydoroxybenzoate preservatives (parabens) are estrogenic. Toxicol Appl Pharmacol 1998;153:12–9.

Routledge EJ, Sumpter JP. Structural features of alkylphenolic chemicals associated with estrogenic activity. J Biol Chem 1997;272:8–3280.

Saikumar P, Dong Z, Mikhailov V, Denton M, Weinberg JM, Venkatachalam MA. Apoptosis: definition, mechanisms, and relevance to disease. Am J Med 1999;107:489–506.

Saunders PT, Fisher JS, Sharpe RM, Millar MR. Expression of oestrogen receptor beta (ER beta) occurs in multiple cell types, including some germ cells, in the rat testis. J Endocrinol 1998;156:13–7.

Shaha C. Modulators of spermatogenic cell survival. Soc Reprod Fertil Suppl 2007;63:173–86.

Song BL, Peng DR, Li HY, Zhang GH, Zhang J, Li KL, et al. Evaluation of the effect of butyl *p*-hydroxybenzoate on the proteolytic activity and membrane function of human spermatozoa. J Reprod Fertil 1991;91:435–40.

Soni MG, Carabin IG, Burdock GA. Safety assessment of esters of phydroxybenzoic acid (parabens). Food Chem Toxicol 2005;43:985–1015.

Tavares RS, Martins FC, Oliveira PJ, Ramalho-Santos J, Peixoto FP. Parabens in male infertility – isthere a mitochondrial connection? Reprod Toxicol 2009;27:1–7.

Taxvig C, Viggaard AM, Hass U, Axelstad M, Boberg J, Hansen PR, et al. Do parabens have the ability to interfere with steroidogenesis. Toxicol Sci 2008;106:206–13.

Tay TW, Andriana BB, Ishii M, Choi EK, Zhu XB, Alam MS, et al. Phagocytosis plays an important role in clearing dead cells caused by mono(2-ethylhexyl) phthalate administration. Tissue Cell 2007;39:241–6.

Tesarik J, Greco E, Cohen-Bacrie P, Mendoza C. Germ cell apoptosis in men with complete and incomplete spermiogenesis failure. Mol Hum Reprod 1998;4:757–62.

vom Saal FS, Cooke P, Buchaman DL, Palanza PP, Thayer KA, Nagel SC, et al. A physiologically based approach to the study of bisphenol A and other estrogenic chemicals on the size of reproductive organs, daily sperm production, and behaviour. Toxicol Ind Health 1998;14:239–60.

Yan W, Suominen J, Samson M, Jegou B, Toppari J. Involvement of Bcl-2 family proteins in germ cell apoptosis during testicular development in the rat and pro-survival effect of stem cell-factor on germ cells in vitro. Mol Cell Endocrinol 2000;165:115–29.

Research Article

Journal of Applied Toxicology

Received: 1 October 2012, Revised: 4 March 2013, Accepted: 4 March 2013 Published online in Wiley Online Library: 10 June 2013

(wileyonlinelibrary.com) DOI 10.1002/jat.2881

In utero and lactational exposure to 2,3,7,8-tetrachlorodibenzo-*p*-dioxin modulates dysregulation of the lipid metabolism in mouse offspring fed a high-calorie diet

Etsuko Sugai[1], Wataru Yoshioka, Masaki Kakeyama, Seiichiroh Ohsako and Chiharu Tohyama*

ABSTRACT: Exposure to environmental chemicals, including dioxins, is a risk factor for type 2 diabetes mellitus in humans. This study explored the hypothesis that *in utero* and lactational exposure to 2,3,7,8-tetrachlorodibenzo-*p*-dioxin (TCDD), the most toxic congener among dioxins, aggravates this disease state later in adulthood. Pregnant C57Bl/6 J mice were administered either a single oral dose of TCDD (3.0 $\mu g\,kg^{-1}$ body weight) or corn oil on gestational day 12.5. The male pups born to these two groups of dams were given either a regular diet or a high-calorie diet, after postnatal day (PND) 28. The four groups of investigated offspring were thus termed T-R (TCDD regular diet), T-H (TCDD high-calorie diet), V-R (vehicle regular diet), and V-H (vehicle high-calorie diet). The mice were regularly monitored for body weight, blood pressure and glucose, until they reached 26 weeks of age. Mice in the V-H group were significantly obese at weeks 15 and 26, but they exhibited no diabetes-associated signs of insulin resistance or hypertension. However, metabolic syndrome-related alterations with marginal signs of liver damage were found at week 26. Pronounced signs of dysregulated lipid metabolism with altered gene expression and liver inflammation were already present at week 15, whereas such alterations were suppressed in the T-H group. Although the mechanism is unclear, this study showed that *in utero* and lactational exposure to low-dose TCDD does not aggravate obesity-induced disease states, such as adult-onset diabetes, but instead attenuates the dysregulation of lipid metabolism brought on by a high-calorie diet. Copyright © 2013 John Wiley & Sons, Ltd.

Keywords: dioxin; environmental chemicals; glucose and lipid metabolism; maternal exposure; mouse

Introduction

The increasing prevalence of diabetes and cardiovascular disease in human populations poses a serious social problem in modern societies. Epidemiological studies suggest that not only intrinsic factors (e.g. obesity-based metabolic alterations), but also extrinsic factors [e.g. exposure to environmental chemicals such as dioxins, polychlorinated biphenyls, and dichlorodiphenyltrichloroethane (DDT)], are associated with the pathogenesis of these disease states (Everett *et al.*, 2007; Fierens *et al.*, 2003; Fujiyoshi *et al.*, 2006; La Merrill *et al.*, 2010). For example, epidemiological studies regarding: (i) Vietnam War veterans previously engaged in the spraying operation of a defoliant containing 2,3,7,8-tetrachlorodibenzo-*p*-dioxin (TCDD) (Michalek *et al.*, 1999); (ii) individuals residing in the vicinity of a polychlorinated biphenyl (PCB)-contaminated Superfund site in the USA (Cranmer *et al.*, 2000); and (iii) workers engaged in handling phenoxy herbicides and chlorophenol (Vena *et al.*, 1998), have all suggested that exposure to environmentally relevant levels of dioxins may be a risk factor for diabetes.

Dioxins are chemicals that are formed unintentionally during combustion. They are persistently and ubiquitously present in the environment and accumulate in various food commodities. TCDD is the most toxic congener among this group of chemicals and induces a variety of toxicities, including carcinogenicity, reproductive and endocrine toxicity, developmental neurotoxicity, and immunotoxicity (van den Berg *et al.*, 2006). Wasting syndrome, characterized by poor weight gain in spite of food intake, weight loss, thymic atrophy and hepatic hypertrophy, is a hallmark of exposure to sublethal doses of dioxin in rodents. Furthermore, exposure to high-dose TCDD alters the energy metabolism (including glucose and lipid metabolism) in rodent livers and cultured cells (Pohjanvirta and Tuomisto, 1994). These toxic events are dependent on the presence of the aryl hydrocarbon receptor (AhR) in affected cells and organs. On the other hand, relatively low doses of TCDD reportedly affect energy metabolism and/or cancer susceptibility. Sato *et al.* (2008) found that C57Bl/6 N mice administered a low daily oral dose of TCDD (5–500 $ng\,kg^{-1}$ body weight) for 18 days

*Correspondence to: Chiharu Tohyama, Laboratory of Environmental Health Sciences, Center for Disease Biology and Integrative Medicine, Graduate School of Medicine, The University of Tokyo, 7-3-1 Bunkyo-ku, Tokyo, 113-0033, Japan. Email: mtohyama@mail.ecc.u-tokyo.ac.jp

Laboratory of Environmental Health Sciences, Center for Disease Biology and Integrative Medicine, Graduate School of Medicine, The University of Tokyo, 7-3-1 Bunkyo-ku, Tokyo, 113-0033, Japan

[1]Present address: Center for Advanced Biomedical Sciences, Administration and Technology, Management Center for Science and Engineering, Waseda University, 2-2 Wakamatsu-cho, Shinjuku-ku, Tokyo, 162-8480, Japan

Journal of AppliedToxicology

developed alterations in the expression of genes associated with energy metabolism in an AhR-dependent manner; hence, AhR apparently mediates actions of both high- and low-dose TCDD. Furthermore, La Merrill *et al.* (2010) administered TCDD (1 μg kg^{-1} body weight) to pregnant mice on gestational day 12.5, and then fed the offspring either a high-fat diet or a regular diet, and administered 7,12-dimethylbenz[a]anthracene as a cancer initiator. They found that the incidence of breast cancer was significantly increased in the offspring fed a high-fat diet and given the carcinogen. In addition, a plethora of published works have shown that exposure to exogenous conditions *in utero*, such as nutritional factors and certain environmental chemicals, similarly affects the postnatal development of the fetus so as to increase the risk of disease in adulthood (Bernal and Jirtle, 2010; Newbold *et al.*, 2008; Waterland *et al.*, 2007). However, little is understood regarding the underlying mechanism behind: (i) the interaction between diet and *in utero* and/or lactational exposure to low-dose TCDD that goes on to affect; and (ii) the development of metabolic syndrome and altered expression of genes associated with energy metabolism later in life.

In the present study, we hypothesized that *in utero* and lactational exposure of mice to a dose of TCDD that is too low to exert overt maternal or fetal toxicity may affect the glucose metabolism and aggravate diabetes mellitus in adulthood. However, no physiological changes were observed to support this hypothesis during the present 26-week observation period. Coincidently, we found that offspring fed a high-calorie diet developed a dysregulation in lipid metabolism that was apparently attenuated by *in utero*/lactational exposure to TCDD. Therefore, we investigated possible diet-mediated alterations in gene expression related to lipid metabolism and the influence of TCDD on such alterations.

Materials and Methods

Reagents

TCDD (purity, >99.5%), purchased from Cambridge Isotope Laboratories (Andover, MA, USA), was diluted with corn oil (Wako Pure Chemicals Ind., Osaka, Japan) to prepare an ingestion solution. The corn oil containing 2% n-nonane (Nacalai Tesque, Kyoto, Japan) was used as the vehicle. Human insulin (Humalin R; Eli Lily Japan, K.K., Kobe, Japan), SuperScript III reverse transcriptase (Invitrogen, Carlsbad, CA, USA), SYBR Premix Ex Taq (Perfect Real Time, Takara Bio Inc., Otsu, Japan), an RNeasy Mini Kit (Qiagen K.K., Tokyo, Japan) and DNase I (Qiagen K.K.) were purchased from the manufacturers shown in the parentheses. The primers for the real-time reverse-transcription polymerase chain reaction (RT-PCR) were manufactured by Hokkaido System Science Co. (Sapporo, Japan). Unless otherwise indicated, all other chemicals and reagents were of analytical grade and purchased from Wako Pure Chemical Industries and Nacalai Tesque.

Animals and TCDD Exposure

Pregnant C57Bl/6J mice were purchased from CLEA Japan (Tokyo, Japan) and kept under a controlled temperature (23 ± 1 °C) and humidity (50 ± 10%) on a 12/12 h light–dark cycle in an animal facility of the University of Tokyo. The experimental protocols of animal experiments of this study were approved by the Animal Care and Use Committee of the Graduate School of Medicine of the University of Tokyo. These animals received standard mouse chow (Labo MR Stock; Nihon Nosan Kogyo, Yokohama, Japan) or a high-calorie diet (High-calorie 32; CLEA Japan) and water *ad libitum*. One gram of the high-calorie diet contained 5.07 kcal (20.1% protein, 23.2% carbohydrate and 56.7% fat by total kcal) and that of the regular diet contained 2.31 kcal (32.6% protein, 52.2% carbohydrate and 15.2% fat by total kcal). Pregnant mice were administered by gavage TCDD (3.0 μg kg^{-1} body weight) or corn oil (vehicle) on gestation day (GD) 12.5. This TCDD dosage was selected based on our pilot study result in that no overt maternal or fetal toxicity was induced (data not shown). It has been known that the placental structure of the mouse is developed by 12.5 days of gestation (Malassiné *et al.*, 2003), and this day was selected as the day of dioxin administration. In addition, dioxins administered during gestation have been established to be transferred not only to the fetuses via the placenta, but also to neonates via lactation (Li *et al.*, 1995). Substantial amounts of TCDD were detected in milk remaining in the stomach of newborn pups (Nishimura *et al.*, 2005). All dams were allowed to litter spontaneously. The number of pups per litter was adjusted

Table 1. Primer sequence of genes

Primer	Forward	Reverse
ACOX	AGAGTGGCCTTGACCTCTGA	CCAATGCCACAGACACAGAC
BOX	GCTGCTAAGGCTCACTGCTA	ACGCTGAATCTCTGGTTCGT
Cyclophiln B	TCGGCAAAGTTCTAGAGGGC	TCTGTGGGGATTGACAGG
CYP1A1	GTTACTGGCTCTGGATACCC	GACAATGCTCAATGAGGCTG
CYP1A2	ACTTTGTGGAGAATGTCACCTCAG	TTGAACAGGGCACTTGTGATGTC
CYP4A10	TTTGCCAGAATGGAGAATGG	CTGTTGGTGCTCAGGGTGT
CYP4A14	GACTCTTGGGACAATGGACA	GTTCCTTCCTCTGGCTGGTA
FAS	AGGACTTGGGTGCTGACTACA	TGGATGATGTTGATGATGGA
HADHa	TGACTGCCTGAGTGCCTTG	GGAGTATCTTTCGCATCCTGGTA
LCAD	ATGGCAAAATACTGGGCATC	ACCCGAGCATCCACGTAAG
PPAR-γ2[a]	TTGAGTTTGCTGTGAAGTTCAAT	CAGCAGGTTGTCTTGGATGT
SREBP-1c	GTGGCAAAGGAGGCACTACA	CAGGAGCCGACAGGAAGG.
TNF-α	CACCACCATCAAGGACTCAA	ACAGAGGCAACCTGACCACT

[a]Ogawa *et al.* (2004)

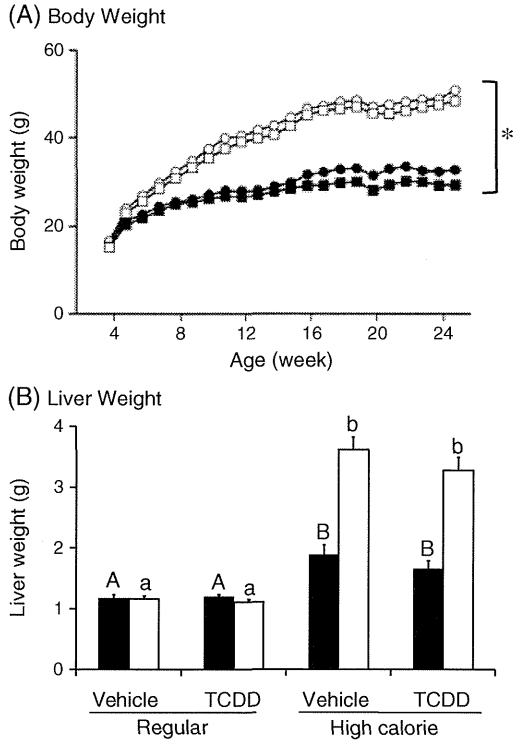

Figure 1. Time courses of body weight (A) and liver weight (B) of mice exposed to 2,3,7,8-tetrachlorodibenzo-*p*-dioxin (TCDD) *in utero* and via lactation, which were fed a regular diet or a high-calorie diet after weaning. Pregnant mice ($n = 9$-10 per group) were administered once by gavage TCDD (3.0 μg kg^{-1} body weight) or corn oil on gestation day (GD) 12.5. The number of litters was adjusted to 6 per dam on postnatal day (PND) 2. From PND 28, male mice were fed either a regular (R) diet or a high-calorie (H) diet, generating four groups ($n = 9$–10 mice per group): (i) vehicle and a regular diet (V-R); (ii) vehicle and a high-calorie diet (V-H); (iii) TCDD and a regular diet (T-R); and (iv) TCDD and a high-calorie diet (T-H). (A) The body weight was significantly different between the high-calorie diet groups (V-H, open circle; T-H, open square) and the regular diet groups (V-R, closed circle; T-R, closed square) from 5 weeks of age, 1 week after feeding the regular or a high-calorie diet by ANOVA with a post hoc test ($P < 0.001$). Asterisks are used to indicate a significant difference of diet. Error bars for each point were too small to be shown in this figure. (B) Liver weight at 15 (closed bar) and 26 (open bar) weeks of age are shown. Differences in the mean of V-R, V-H, T-R and T-H were compared within each age group, and values with different letters (uppercase and lowercase letters for 15 and 26-week-old mice, respectively) indicate a statistically significant difference from each other at $P < 0.05$. No statistical comparison was performed between the V-R and T-H groups, or between the T-R and V-H groups.

to 6 on postnatal day (PND) 2 to minimize the possible effects owing to the litter size. The majority of the pregnant mice delivered 6–11 pups per litter. However, we had pregnant mice that had three to five pups at birth, foster pups from dams that had more than 6 pups at birth and all the pregnant mice nursed a total of 6 pups.

On PND 28, the body weight of male pups born to dams given TCDD or corn oil was measured and the male pups of each treatment group were subdivided into two more groups (regular diet and high-calorie diet). Thus, four groups of pups were used in this study: Group 1 with vehicle and a regular diet (referred to as V-R, thereafter), $n = 20$ from 10 dams; Group 2 with vehicle and a high-calorie diet (V-H), $n = 20$ from 9 dams; Group 3 with TCDD and a regular diet (T-R), $n = 21$ from 8 dams; Group 4 with TCDD and a high-calorie diet (T-H), $n = 22$ from 10 dams.

Monitoring of Health Conditions and Glucose Tolerance and Insulin-resistant Tests

During the experimental period, the body weight and food intake of mice born to dams given vehicle or TCDD were monitored once a week until week 26. Blood pressure was determined using a Blood Pressure Monitor (Model MK-2000ST, Muromachi Kikai Co, Tokyo, Japan) at 9, 19 and 23 weeks after birth.

The glucose tolerance test (GTT) and the insulin resistance test (IRT) were carried out according to methods reported by Terauchi *et al.* (1997), with some modifications. For the GTT, male mice (12 and 20 weeks old) were subjected to fasting for 13 h before the test. They were then injected intraperitoneally (i.p.) with glucose (1.5 mg g^{-1} body weight). Blood was taken from the tail vein at 0, 30, 60, 120 and 180 min after the glucose injection. Blood glucose levels were determined using a Fuji Dri-Chem7000V Veterinary Chemistry Analyzer (Fujifim Medical Co., Tokyo, Japan). For the IRT, male mice (13 and 21 weeks old) were fed *ad libitum* and then subjected to fasting during the test. They were i.p. challenged with human insulin (0.75 mU g^{-1} body weight). Blood was drawn from the tail vein at 0, 30, 60, and 90 min after insulin injection, and blood glucose levels were determined as described above.

Collection of Blood and Liver Tissues

After overnight fasting, 9 and 11–13 mice from each group were autopsied under diethyl ether anesthesia in the 15th and 26th weeks after birth, respectively. Blood was collected from the abdominal vein during autopsy, followed by the separation of serum for blood analyzes, and liver tissues were collected, snap-frozen in liquid nitrogen and stored at –80 °C until gene expression analyzes.

Real-time RT-PCR

For the analysis of gene expression by real-time RT-PCR, six liver tissues were randomly selected from nine 15-week-old and eleven 26-week-old mice. Total RNA was extracted using RNeasy according to the manufacturer's instructions and purified to obtain a DNase I-digested RNA specimen using an RNeasy Mini column. First-strand cDNA synthesis was carried out with the Super Script III First-Strand Synthesis System for real-time RT-PCR. Total RNA samples (1 μg) were denatured for 5 min at 65 °C with 2.5 μM oligo(dT_{20}), primer and reverse-transcribed with 200 U of Superscript III RT, 0.5 mM dNTP mix and 5 mM dithiothreitol for 50 min at 55 °C, and 10 min at 50 °C, followed by a termination reaction for 15 min at 70 °C. The volume of the reaction mixture for reverse transcription was 20 μl. Quantitative RT-PCR analysis was performed using a LightCycler (Roche Diagnostics K.K., Tokyo, Japan) and SYBR Premix Ex Taq (Perfect Real Time) according to the manufacturer's protocol. The primer sets of genes used in the present study are summarized in Table 1. These genes include acetyl-CoA carboxylase (ACC), acyl-CoA oxidase (ACOX), branched-chain acyl-CoA oxidase (BOX), cyclophiln B

Journal of Applied Toxicology

Table 2. Blood pressure (mmHg) and heart rate (beats per min) in mice born to dams exposed to 2,3,7,8-tetrachlorodibenzo-*p*-dioxin (TCDD) or vehicle[a]

	Regular diet				High Calorie diet			
Age	Vehicle		TCDD		Vehicle		TCDD	
(Week)	BP (mmHg)	Heart rate (beats per min)	BP (mmHg)	Heart rate (beats per min)	BP (mmHg)	Heart rate (beats per min)	BP (mmHg)	Heart rate (beats per min)
9	100 ± 7	671 ± 28	104 ± 2	713 ± 11	102 ± 1	718 ± 33	99 ± 4	740 ± 4
19	108 ± 5	690 ± 16	109 ± 3	711 ± 6	98 ± 7	706 ± 11	111 ± 5	726 ± 12
23	116 ± 2	707 ± 3	122 ± 3	728 ± 10	125 ± 4	717 ± 8	125 ± 4	729 ± 6

[a]Data were analyzed on a litter-by-litter basis, using two-way ANOVA to analyze the effects of diet and exposure. The number of dams was 6, 7 or 8 per each group. No differences in systolic blood pressure and heart rate were found.

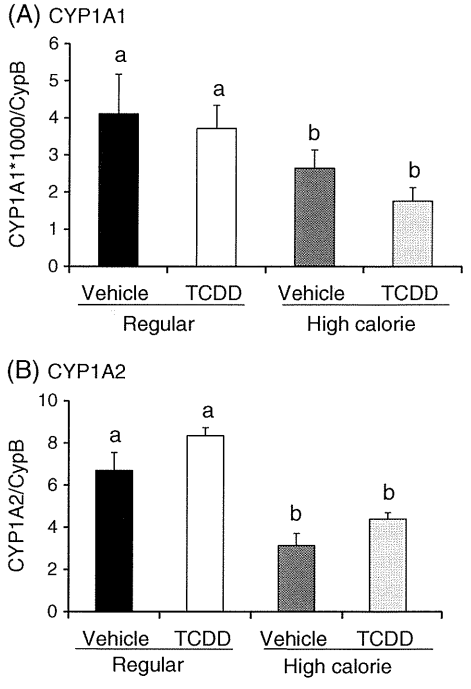

Figure 2. CYP1A1 and CYP1A2 mRNA expression in the liver of 15-week-old mice exposed to 2,3,7,8-tetrachlorodibenzo-*p*-dioxin (TCDD) *in utero* and via lactation, and fed a high-calorie diet or a regular diet after weaning. The group classification is the same as that in Fig. 1. RNA was extracted from the liver. At least one mouse was randomly selected from a litter, and 4–5 litters out of 9 dams were also randomly selected for each group. After the preparation of RNA from the liver, quantitative RT-PCR was performed to determine the CYP1A1 and CYP1A2 mRNA expression levels relative to that of CypB mRNA. Data are shown as the mean ± SE ($n = 4$–5 per group). No statistical comparison was performed between the V-R and T-H groups, or between the T-R and V-H groups.

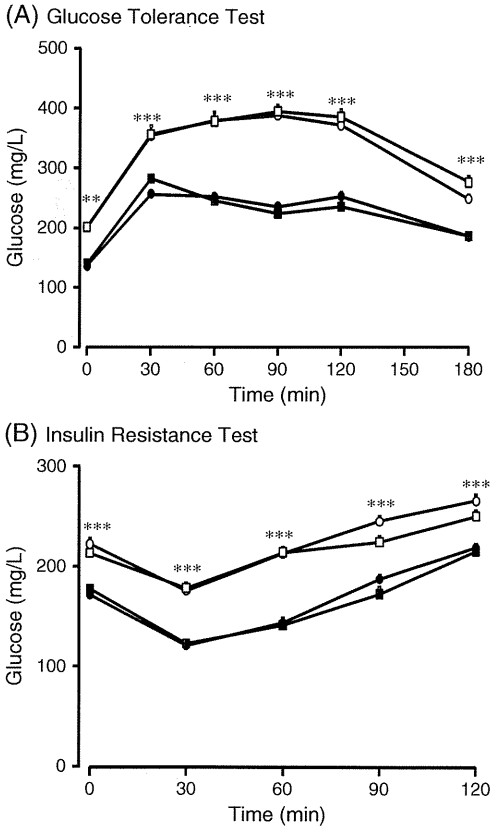

Figure 3. Glucose tolerance test (A) and insulin resistant test (B) in mice exposed to 2,3,7,8-tetrachlorodibenzo-*p*-dioxin (TCDD) *in utero* and via lactation, which were fed a high-calorie diet or a regular diet after weaning. The group classification is the same as that in Fig. 1. The glucose tolerance test and insulin resistance test were performed in 20-week-old mice ($n = 7$–8 per group) and 21-week-old mice ($n = 7$–8 per group), respectively. In the both tests, two-way ANOVA with post hoc analysis indicates that there is a significant main effect of diet (P 0.001), but not of exposure, for blood glucose levels, and that they were significantly higher in the high-calorie diet groups (V-H, open circle; T-H, open square) than in the regular diet groups (V-R, closed circle; T-R, closed square). Asterisks indicate a statistically significant difference at $P < 0.01$ (**) and 0.001 (***). No statistical comparison was performed between the V-R and T-H groups, or between the T-R and V-H groups.

(CypB), CYP1A1, CYP4A10, CYPA14, fatty acid synthase (FAS), long-chain acyl-CoA dehydrogenase (LCAD), long-chain L-3-hydroxyacyl-coenzyme A dehydrogenase α (HADHα), peroxisomal proliferator-activated receptor PPAR-γ2, sterol regulatory element-binding protein (SREBP-1c) and tumor necrosis factor TNF-α. The amplification program is described as follows: one cycle of 95 °C for 10 s, followed by 40 cycles of denaturation for 5 s at 95 °C, annealing of primers for 20 s at 60 °C and extension for 15 s at 65 °C. After completion, a melting curve analysis was performed to monitor PCR

